Exhibit A

Role of oxygen in biodegradation of poly(etherurethane urea) elastomers

Mark A. Schubert,[1] Michael J. Wiggins,[1] James M. Anderson,[1,2] and Anne Hiltner[1,*]
[1]Department of Macromolecular Science and [2]Institute of Pathology, Case Western Reserve University, Cleveland, Ohio 44106

It is generally accepted that biodegradation of poly(etherurethane urea) (PEUU) involves oxidation of the polyether segments on the surface where leukocytes are adhered. The influence of dissolved oxygen, which is known to control oxidation of polymers in more traditional environments, was explored in this study. Specimens treated *in vitro* with hydrogen peroxide–cobalt chloride for 12 days exhibited a brittle, degraded surface layer about 10 μm thick. Attenuated total reflectance–Fourier transform infrared spectroscopy of the surface revealed that the ether absorbance at 1110 cm^{-1} gradually decreased with *in vitro* treatment time to 30% of its initial value after 12 days. In contrast, 6 days *in vitro* followed by 6 days in air produced a decrease to 12% of the initial volume. Therefore, removing a specimen from the *in vitro* solution after 6 days and exposing it to air for the remainder of the 12 days actually resulted in more oxidation than leaving it in the *in vitro* solution for the entire 12 days. These results suggest that PEUU degrades by an auto-oxidation mechanism sustained by oxygen. By successfully modeling the depth of the surface degraded layer with a diffusion-reaction model, it was demonstrated that PEUU biodegradation is controlled by diffusion of oxygen into the polymer. © 1997 John Wiley & Sons, Inc.

INTRODUCTION

The revelation that polyetherurethane elastomers undergo environmental stress cracking during human implantation[1] has stimulated extensive research directed toward identifying the mechanisms of this undesirable phenomenon.[2–8] It is now generally accepted that the primary chemical mechanism involves surface oxidation of polyether segments at sites of leukocyte adhesion.[6,7] The *in vivo* degradation can be reproduced *in vitro* with a hydrogen peroxide–cobalt chloride system.[2,3,5] Hydrogen peroxide and cobalt ion undergo a Haber–Weiss reaction to create reactive hydroxyl radicals:

$$Co^{++} + H_2O_2 \rightarrow Co^{+++} + HO^- + HO\cdot \qquad (1)$$

Hydroxyl radicals subsequently initiate oxidation by abstracting an α-methylene hydrogen atom from the poly(etherurethane urea) (PEUU) ether[3,5,8]:

$$-CH_2-O-CH_2- + HO\cdot \rightarrow -\dot{C}H-O-CH_2- + H_2O \qquad (2)$$

*To whom correspondence should be addressed.

It is proposed that chain scission occurs by radical–radical combination of the alkyl-polymer radical and another hydroxyl radical with formation of a hemiacetal.[3] Rearrangement of the hemiacetal causes chain scission and produces aldehyde and alcohol end groups:

$$\begin{aligned} -CH_2-\dot{C}H-O-CH_2- + HO\cdot &\rightarrow -CH_2-CH(OH)-O-CH_2- \\ &\downarrow H_2O,H^+ \\ -CH_2-OH + HO-CH(OH)-O-CH_2- &\rightleftharpoons O{=}CH-O-CH_2- + H_2O \end{aligned} \qquad (3)$$

This mechanism does not consider the influence of dissolved oxygen. Molecular oxygen frequently controls oxidation of polymers in more traditional environments by sustaining auto-oxidation.[9–11] The possibility that oxygen has a similar role in biodegradation of PEUUs has been explored with additional *in vitro* experiments.

Journal of Biomedical Materials Research, Vol. 34, 519–530 (1997)

CCC 0021-9304/97/040519-12

EXPERIMENTAL

Materials

The PEUU was used in previous studies and is fully described elsewhere.[12] The PEUU consists of a poly(tetramethyleneglycol) soft segment (M_n = 2000) and a methylene di(*p*-phenyl isocyanate) hard-segment chain extended with diamines. The number average molecular weight of the PEUU is approximately 40,000, determined by gel permeation chromatography, relative to polystyrene standards. PEUU films 0.5 mm thick were cast from a dimethyl acetamide solution (20% solids, wt./wt.) onto glass petri dishes. The solvent was removed by drying in vacuum at room temperature for 3 days.

In vitro treatments

Unstrained PEUU films, approximately 5 × 5 cm, were treated *in vitro* with 100 mL 20% H_2O_2/0.1 *M* $CoCl_2$ at 37°C for 12 days. The treatment solution was changed every 3 days. Films were prevented from floating to the surface of the treatment solution by weighting with glass rods.

Characterization

Immediately before and after treatment specimens were analyzed by attenuated total reflectance–Fourier transform infrared (ATR-FTIR) spectroscopy (Nicolet® 800 FT-IR spectrometer). The ATR attachment (Harrick Scientific, Inc.) used an optical angle of 60° and a germanium crystal with an endface angle of 60°. Spectra were collected at a resolution of 2 cm^{-1} for 300 scans. Oxidation of polyether was measured from the peak height of the amorphous aliphatic ether absorbance at 1110 cm^{-1}, ν(C—O—C).[13] Peak heights were normalized to the aromatic carbon–carbon stretch at 1591 cm^{-1}. To examine the effect of swelling by hydrogen peroxide, a PEUU film was cast onto a KBr disk 1 cm in diameter. Transmission FTIR spectroscopy was performed on the dry film. Approximately 2 mL of hydrogen peroxide (30%) was placed on the PEUU film for 15 min at room temperature and then removed. The transmission FTIR spectrum of the swollen film was obtained immediately. The film was again analyzed after drying 10 min in the IR sample chamber.

A Varian DS-651 Star System with a 9010 Solvent Delivery System and a 9065 Polychrom® ultraviolet (UV) diode-array detector was employed for gel permeation chromatography analysis. The eluent was tetrahydrofuran (THF) with a flow rate of 1.0 mL/min at 40°C. Three columns of highly crosslinked polystyrene–divinylbenzene (PLGel; Polymer Laboratories, Inc.) with pore sizes of 500, 10^4, and 10^5 Å were used for separation. The PEUU specimens were dissolved in THF at 0.1 *M* LiCl and the UV absorbance at 254 nm was used for detection.

Scanning electron micrographs (SEM) were acquired with a JEOL® 840-A scanning electron microscope. All samples were vacuum dried at room temperature and coated with 90 Å of gold prior to scanning.

The diffusion of oxygen through PEUU was measured at 37°C and 90% relative humidity with a Ox-Trans® 2/20 oxygen permeability tester (MOCON®; Modern Controls, Inc., Minneapolis, MN). The diffusion of cobalt into PEUU was investigated by placing an 8 × 12 cm, 12-μm-thick PEUU film in a diffusion cell. One side of the cell contained 280 mL of 20% hydrogen peroxide in 0.5 *M* cobalt chloride; the other

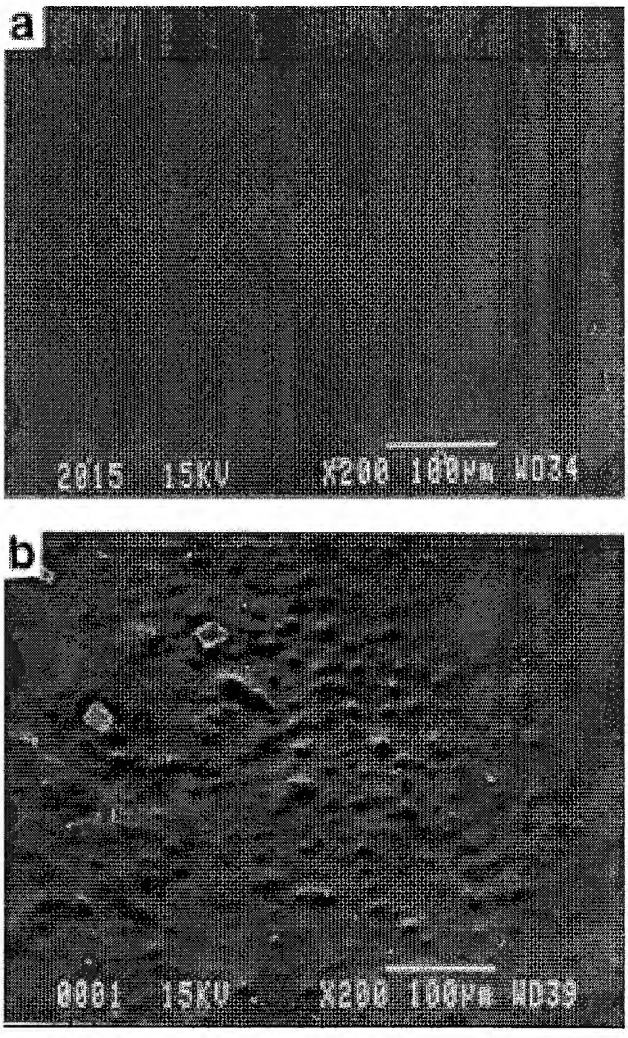

Figure 1. SEM micrographs of PEUU at 60° tilt. **(a)** Untreated and **(b)** treated 12 days *in vitro*.

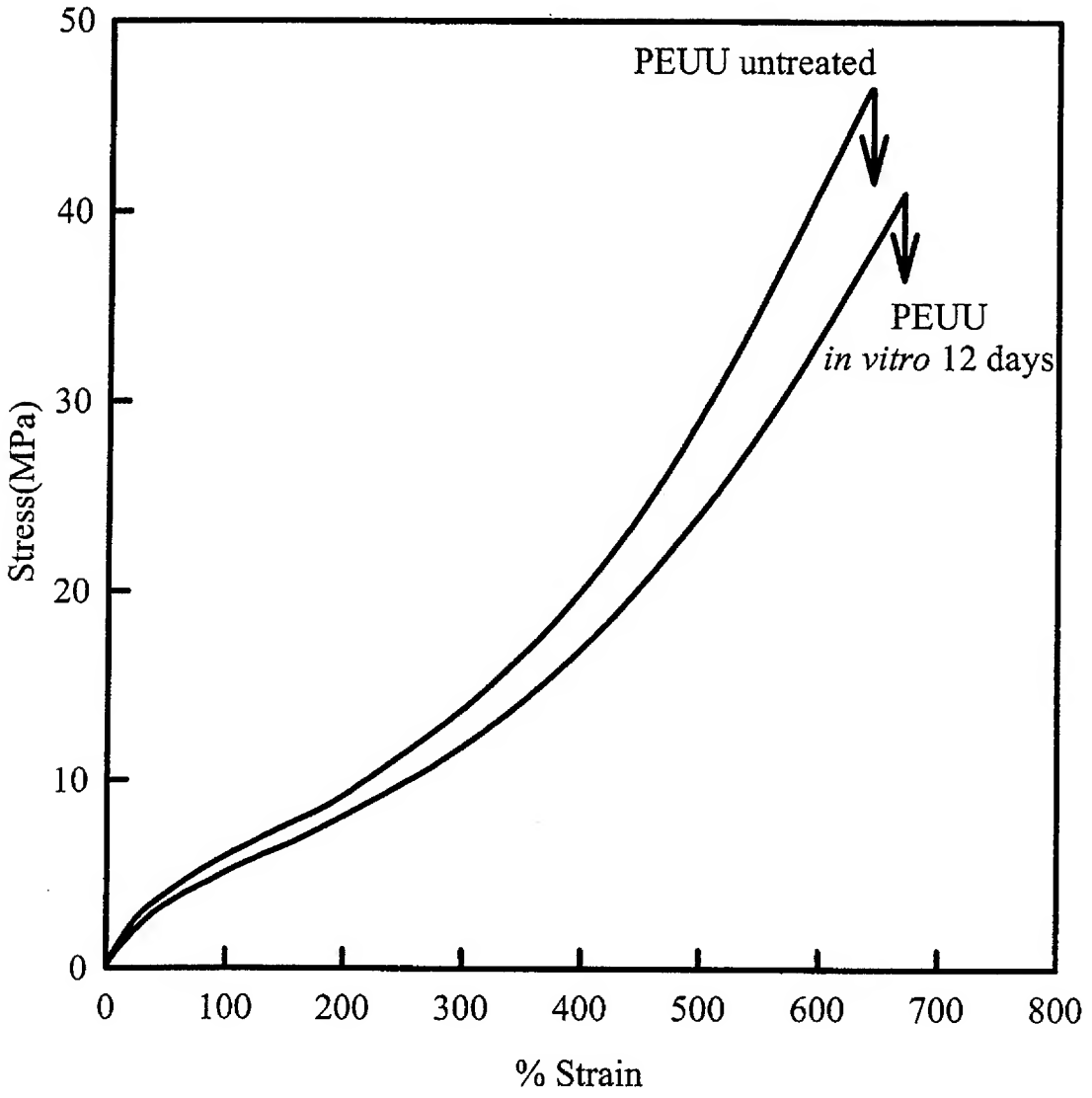

Figure 2. Tensile stress-strain curves for untreated PEUU film and PEUU film treated 12 days *in vitro*.

side contained 280 mL 0.5 *M* magnesium chloride to equilibrate the osmotic gradient.

Stress-strain measurements of 0.5-mm-thick PEUU films were performed using ASTM 1708 D specimen geometry with a strain rate of 100 mm/min.

RESULTS AND DISCUSSION

In vitro treatments

Before treatment, the surface of the PEUU film was smooth and featureless [Fig. 1(a)]. After 12 days *in vitro*, the surface exhibited roughening and dimpling but no pitting or cracking. In contrast, biaxially and uniaxially strained PEUU films treated in this *in vitro* system exhibited extensive pitting and cracking.[2,3,5] Assuming that chemical degradation by oxidative chain scission occurs on both strained and unstrained PEUU, the differences are attributed to the effects of strain on subsequent events. Pits form when areas of localized chain scission open up as a result of the stress in the material. With time, small pits 1–20 μm in diameter coalesce into larger pits and cracks.[2,3,5] The pitting and cracking do not occur in treated films if they are not strained during treatment.

Stress-strain relationships for the PEUU films revealed a 10% decrease in stress after 12 days *in vitro* (Fig. 2). Otherwise, the shape of the curve and the strain at fracture were not affected. The residual strain after 24 h at room temperature was the same, about 2%, for both untreated and treated specimens. Although the 12-day *in vitro* treatment had only a moderate effect on the bulk mechanical properties, SEM of the fractured specimen revealed a brittle, profusely cracked surface [Fig. 3(a)]. Tilting the specimen to expose the fracture plane revealed a crack depth of 10–15

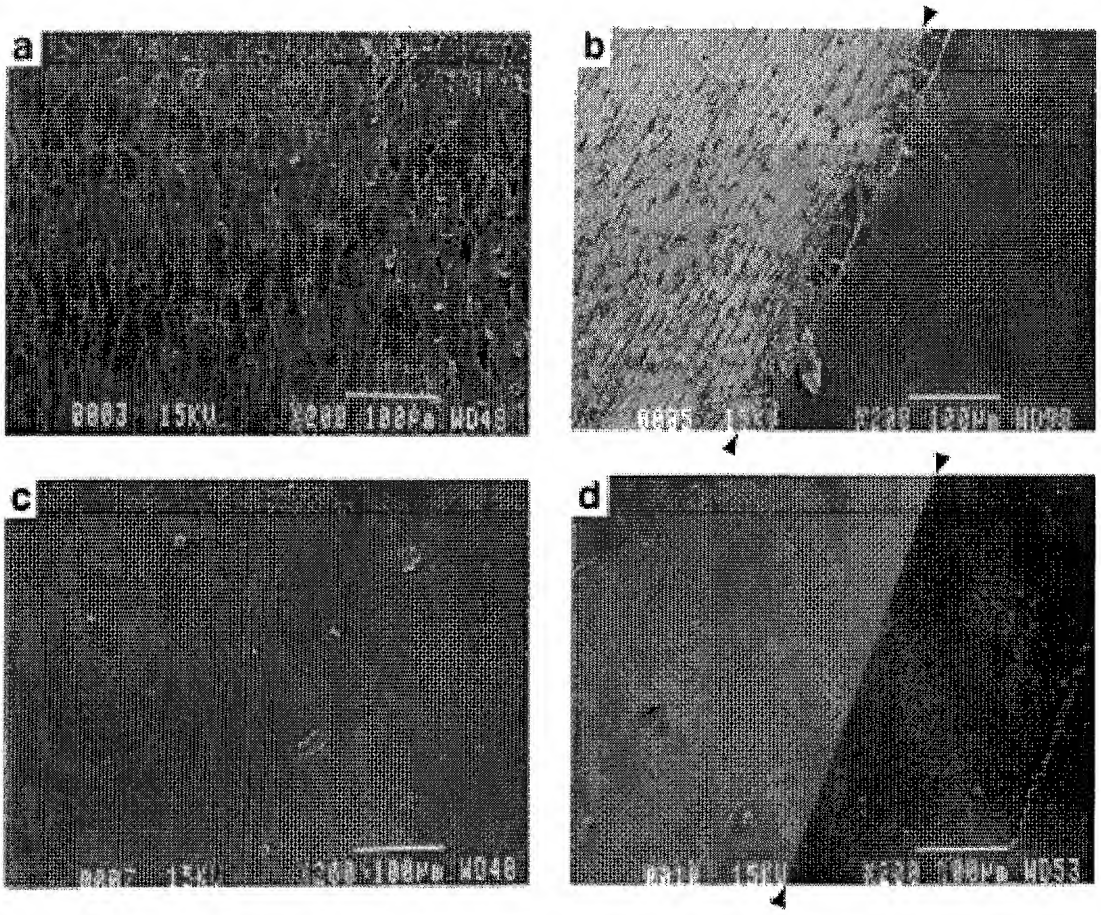

Figure 3. SEM micrographs of PEUU film strained to fracture. **(a)** Treated 12 days *in vitro*, **(b)** fracture plane of the 12-day *in vitro* treated specimen, **(c)** untreated, and **(d)** fracture plane of the untreated specimen. Arrows in **(b)** and **(d)** locate the corner formed by the film surface and the fracture plane.

μm with no apparent degradation in the bulk [Fig. 3(b)]. In contrast, the surface and fracture plane of the untreated PEUU film did not show any physical damage after straining to fracture [Fig. 3(c,d)]. The depth of the cracked layer is consistent with previous studies. Creep studies on PEUU in the same *in vitro* environment also indicated a degradation depth of 10 μm.[14] Furthermore, the depth of chemical degradation was reported to be 10 μm in an ATR-FTIR study of PEUU implanted for 10 weeks.[6] It can be speculated that some of the brittle cracking of PEUU that has been described in the literature was caused by the handling of explanted specimens during retrieval and characterization.[1,2,4,6–8]

The surface specificity of PEUU degradation suggested that oxidation was controlled by diffusion of one or more degradative species. Following current understanding of the PEUU biodegradation mechanism, candidate species include hydrogen peroxide, cobalt ion, and hydroxyl radicals produced by the cobalt-catalyzed dissociation of hydrogen peroxide. It is known that pure water swells PEUU 1.1% (equilibrium) by weight, and in the *in vitro* environment, PEUU swells 6.7% (equilibrium) by weight within several minutes.[14] Therefore, both water and hydrogen peroxide are available throughout the bulk of the PEUU during *in vitro* treatment. Transmission FTIR spectra were collected from untreated PEUU and PEUU swollen in 30% hydrogen peroxide (Fig. 4). The shift in the ether stretch at 1110 cm^{-1} to lower frequencies indicates the presence of water and/or hydrogen peroxide in the soft-segment phase hydrogen bonded to the ether oxygen. These spectra also show an increase in hydrogen-bonded urethane carbonyls by the decrease in the 1730-cm^{-1} free urethane carbonyl absorbance and the increase in the 1709-cm^{-1} hydrogen-bonded urethane carbonyl. The hard-segment urea carbonyl at 1637 cm^{-1} is hydrogen bonded before swelling and no effect by hydrogen peroxide could be measured. All the spectral changes were reversed by drying the PEUU film.

No diffusion of cobalt through a 12-μ-thick PEUU film was detected by UV-vis spectroscopy after six days at 37°C. Additionally, x-ray dispersion analysis of the surface and cross section of a PEUU film treated for 12 days in the 20% hydrogen peroxide 0.1 *M* cobalt chloride system did not detect any cobalt. Therefore, it is assumed that cobalt does not diffuse into the PEUU

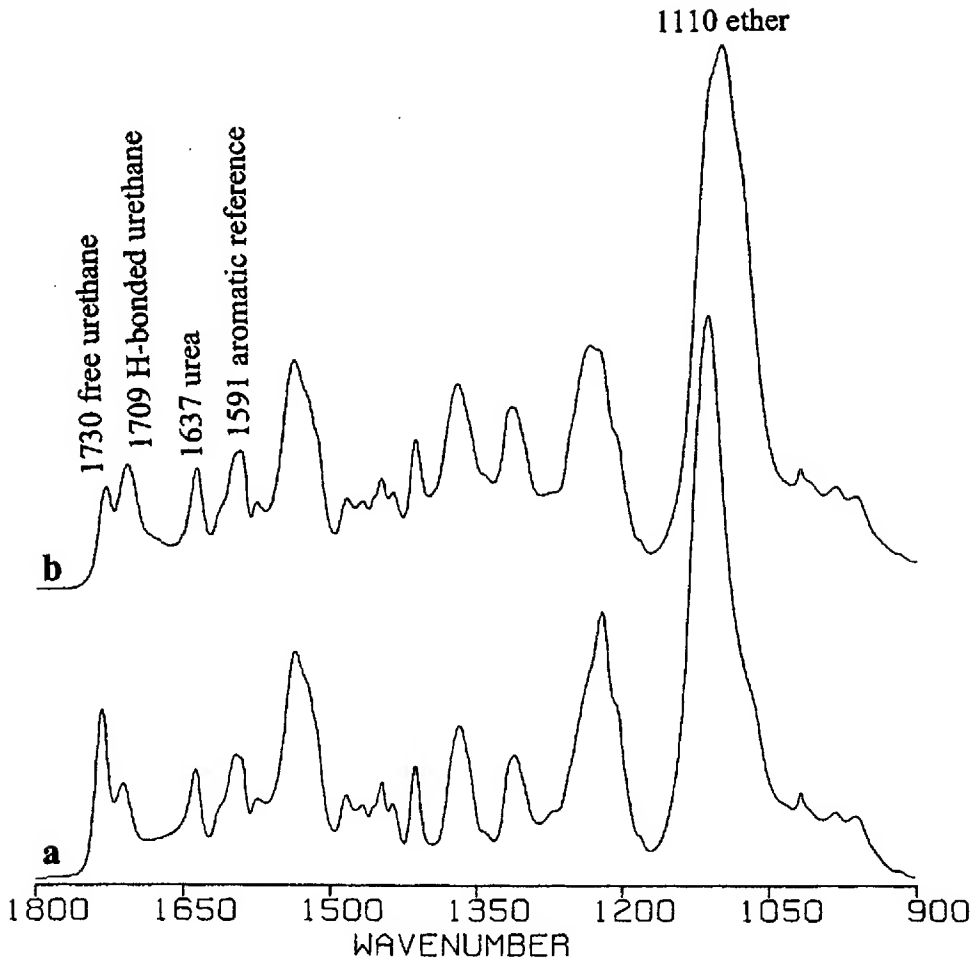

Figure 4. Transmission FTIR spectra. **(a)** Untreated PEUU, and **(b)** PEUU swollen in 30% hydrogen peroxide for 15 min.

in significant levels and does not catalyze the decomposition of hydrogen peroxide in the bulk PEUU.

If cobalt is not available within the PEUU to catalyze decomposition of hydrogen peroxide, hydroxyl radicals must diffuse into the PEUU from the surrounding *in vitro* solution. Hydroxyl radicals are vigorously reactive, with rate constants on the order of $10^9\ M^{-1}\ s^{-1}$,[15] and might be expected to react at the PEUU surface immediately after formation.[16] The presence of hydrogen peroxide and water in the PEUU offers several pathways by which radicals can transfer rapidly into the PEUU from the surface. It is known that the hydroxyl radical transfers by reaction with water[17,18]:

$$HO\cdot + H_2O \rightarrow H_2O + HO\cdot \quad (4)$$

It is also possible that the hydroxyl radical can transfer by an analogous reaction with hydrogen peroxide:

$$HO\cdot + H_2O_2 \rightarrow H_2O_2 + HO\cdot \quad (5)$$

Alternatively, the hydroxyl radical can transfer with hydrogen peroxide to create a hydroperoxy radical [Eq. (6[a])].[19] The hydroperoxy radical can react with another hydrogen peroxide to regenerate the hydroxyl radical [Eq. (6[b])]:

$$HO\cdot + H_2O_2 \rightarrow H_2O + HOO\cdot \quad (6a)$$

$$HOO\cdot + H_2O_2 \rightarrow H_2O + O_2 + HO\cdot \quad (6b)$$

The hydroperoxy radical found in Equation (6[a]) can also abstract an α-methylene hydrogen from the PEUU ether. This can subsequently lead to chain scission following a mechanism previously proposed for *in vivo* oxidation.[5] Therefore, it is reasonable to assume that hydroxyl radicals and possibly hydroperoxy radicals are available in the PEUU to initiate oxidation by hydrogen abstraction from ether methylenes. Hydrogen peroxide can also act as a chain transfer agent for the proposed oxidation mechanism[20]:

$$—\dot{C}H—O— + H_2O_2 \rightarrow —CH_2—O— + HOO\cdot \quad (7a)$$

$$HOO\cdot + H_2O_2 \rightarrow H_2O + O_2 + HO\cdot \quad (7b)$$

Oxygen dependence

Oxygen is a reactive specie present *in vitro* and *in vivo*. A series of experiments was carried out to deter-

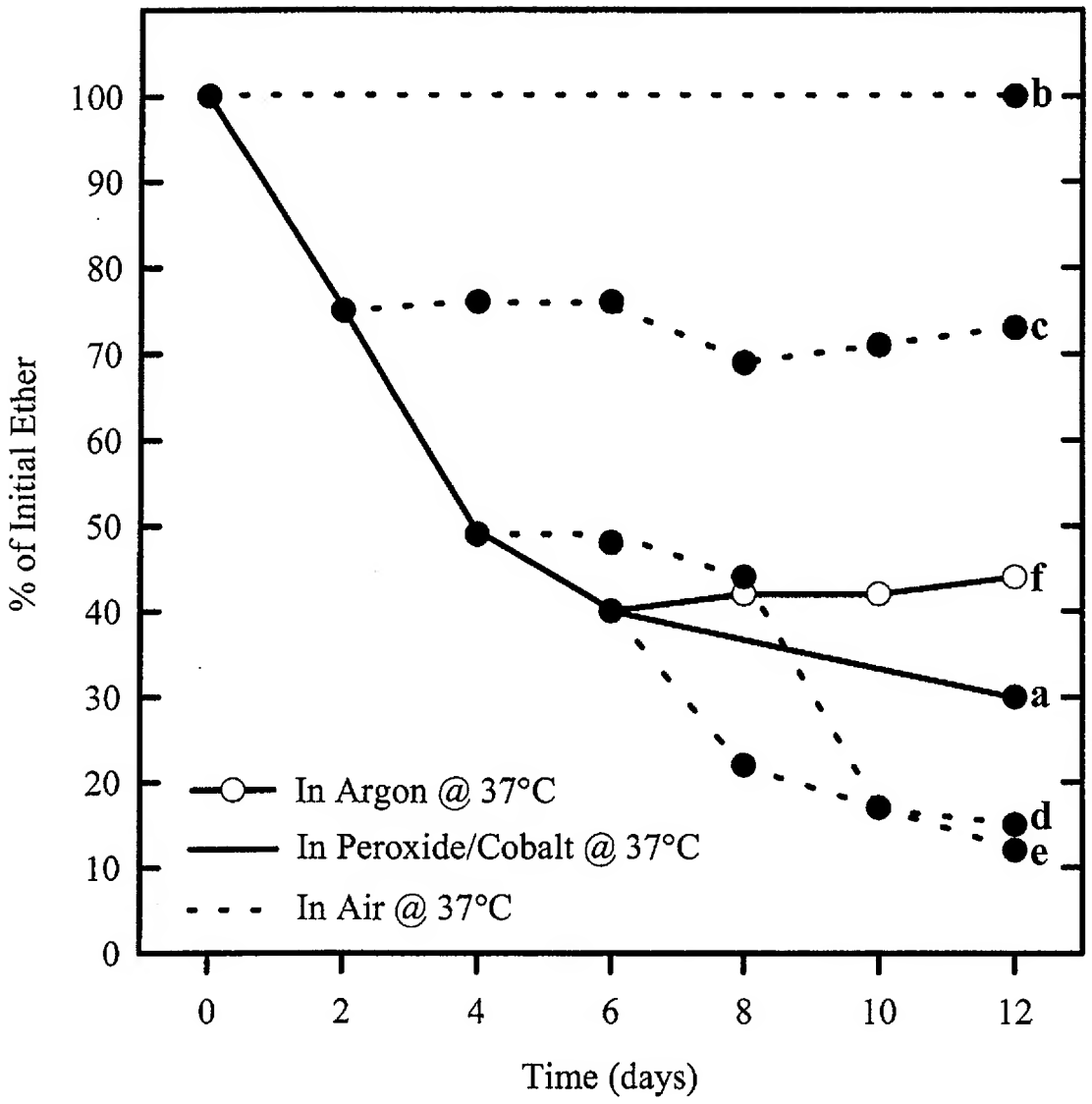

Figure 5. ATR-FTIR peak height analysis of polyether absorbance at 1110 cm^{-1} ν(C—O—C). Percent initial ether = $(A_{1110}/A_{1591})_{treated}/(A_{1110}/A_{1591})_{untreated} \times 100\%$.

mine the sensitivity of PEUU degradation to oxygen. Specimens were treated *in vitro* for 0, 2, 4, or 6 days and then without rinsing placed in air (oxygen concentration 0.20 ml/ml · atm) or argon at 37°C for the remainder of the 12-day treatment. The ATR-FTIR ether absorbance at 1110 cm^{-1} gradually decreased with *in vitro* treatment time (curve a in Fig. 5). If the PEUU was not exposed to the *in vitro* treatment or was exposed for only 2 days, no change in the ether occurred during subsequent exposure to air (curves b and c). In contrast, after 4 days *in vitro*, the ether peak height subsequently remained constant for the first 4 days in air but then decreased from 50% to 15% during the final 4 days in air (curve d), and after 6 days *in vitro*, the ether peak height decreased from 40% to 12% during 6 days in air (curve e). However, placing the specimens in argon after 6 days *in vitro* resulted in no further degradation (curve f). Removing the specimens from the *in vitro* solution after 4 or 6 days and exposing them to air for the remainder of the 12 days actually resulted in more degradation than leaving them in the *in vitro* solution for the entire 12 days.

Representative ATR-FTIR spectra of the carbonyl stretching region in Figure 6 reveal other features of the degradation. In addition to decreases in urethane carbonyl absorptions at 1730 and 1709 cm^{-1}, there is a change in shape in the carbonyl region of the specimens treated 6 days *in vitro* plus 6 days in air compared to the specimens treated *in vitro* for 12 days. The valley between the 1730 and 1709 cm^{-1} disappeared; spectral subtraction revealed a new broad carbonyl at 1716 cm^{-1} which corresponds to a carboxylic acid carbonyl-stretching absorbance. In addition, a hydroxyl stretching, ν(O—H), absorbance near 3300 cm^{-1} confirmed the presence of carboxylic groups.

The proposed oxidative mechanism of polyether

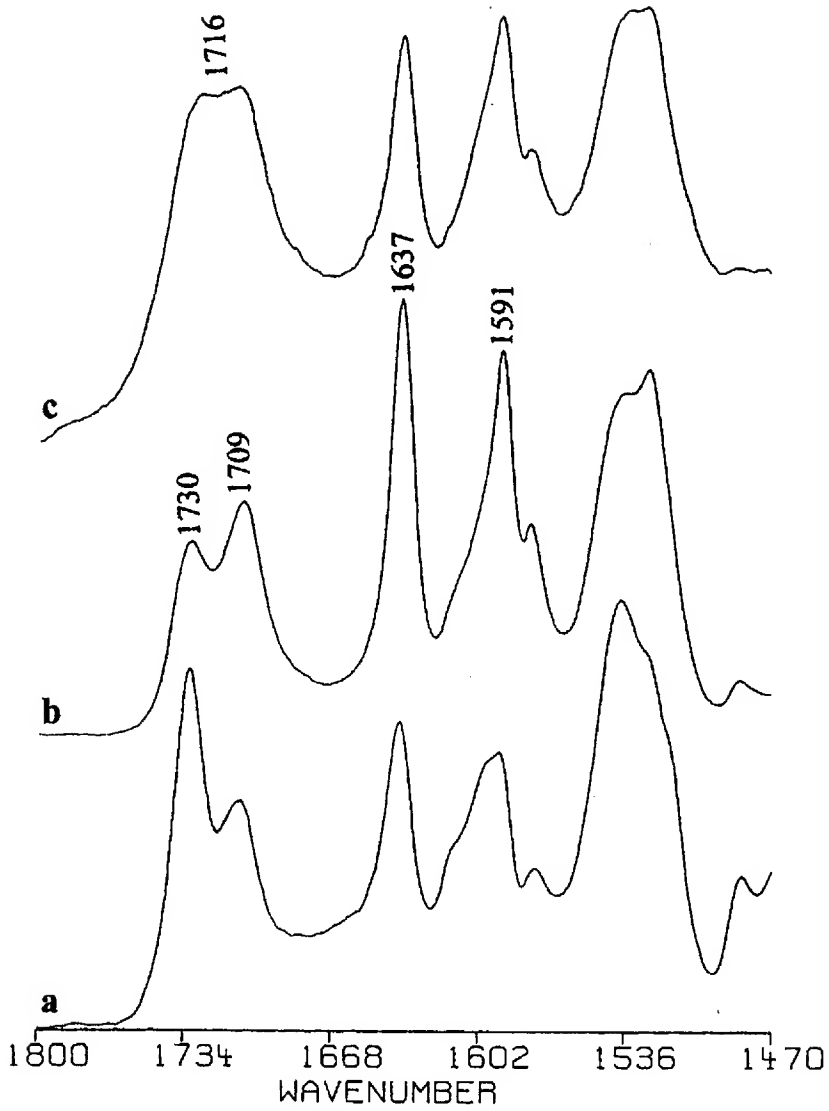

Figure 6. ATR-FTIR spectra of PEUU. **(a)** Untreated, **(b)** treated 12 days *in vitro*, and **(c)** treated 6 days *in vitro* followed by 6 days in air.

degradation leads to products with carboxylic acid, aldehyde, and alcohol moities.[3,6] Previously, the absence of these absorbances in ATR-FTIR spectra of degraded PEUU was attributed to extraction of the low-molecular-weight degradation products into the solution (*in vitro*) or exudate (*in vivo*).[3] When degradation occurred in air, where degradation products could not be extracted, the oxygen-containing species were found. Additional evidence for extraction of acidic degradation products during *in vitro* treatment was the appearance, after 5 days *in vitro*, of an organic surface layer on the treatment solution that could have been the oxidative degradation products of PEUU. Furthermore, the pH of the *in vitro* solution decreased from 3.62 ± 0.01 to 3.14 ± 0.05 (n = 3) after 12 days of PEUU treatment, apparently owing to the presence of acidic degradation products, because in the absence of the PEUU the pH of the solution increased slightly to 3.70 ± 0.05 (n = 3) after 12 days.

Molecular weight distribution by gel permeation chromatography (GPC) was also different in specimens treated 6 days *in vitro* followed by air treatment for 6 days compared to specimens treated 12 days *in vitro* (Fig. 7). After both treatments, the chromatograms broadened compared to the chromatogram of untreated PEUU and polydispersity increased from 2.0 for the untreated PEUU to 2.6 for the 6-day *in vitro* and 6-day air-treated specimens and 2.7 for the 12-day *in vitro*-treated specimens. However, the chromatogram of the specimen treated 6 days *in vitro* followed by 6 days in air also shifted to a longer elution time indicating a decreased peak molecular weight (Table I).

Auto-oxidation of PEUU

The solubility of oxygen in water is 0.02 ml/ml · atm and may be lower in the aqueous *in vitro* solution

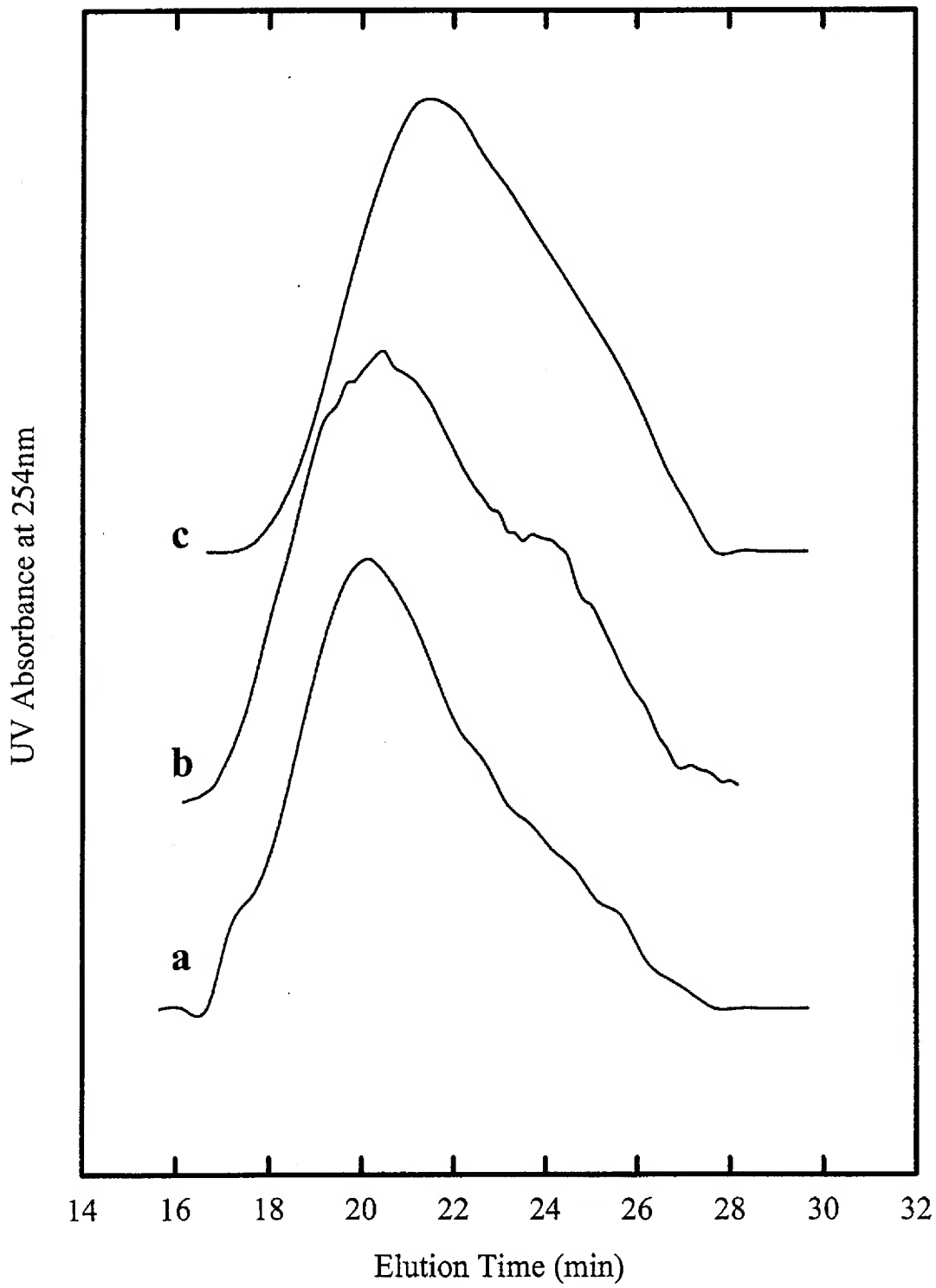

Figure 7. Gel permeation chromatographs of PEUU. **(a)** Untreated, **(b)** 12 days *in vitro,* and **(c)** 6 days *in vitro* followed by 6 days in air.

owing to the "salting-out" effect of the cobalt chloride and hydroxyl ions from the decomposition of hydrogen peroxide.[21] It seems reasonable to assume that the solubility of oxygen *in vitro* is approximately 0.01 ml/ml · atm. The increased rate of oxidation when oxygen concentration increased from 0.01 ml/ml · atm (*in vitro*) to 0.20 ml/ml · atm (air), and evidence of an induction period suggest that PEUU degradation follows a classical auto-oxidation process. As shown schematically in Figure 8, degradation initiates with the formation of alkyl radicals on the polymer chain. In the presence of oxygen, the polymer alkyl radical

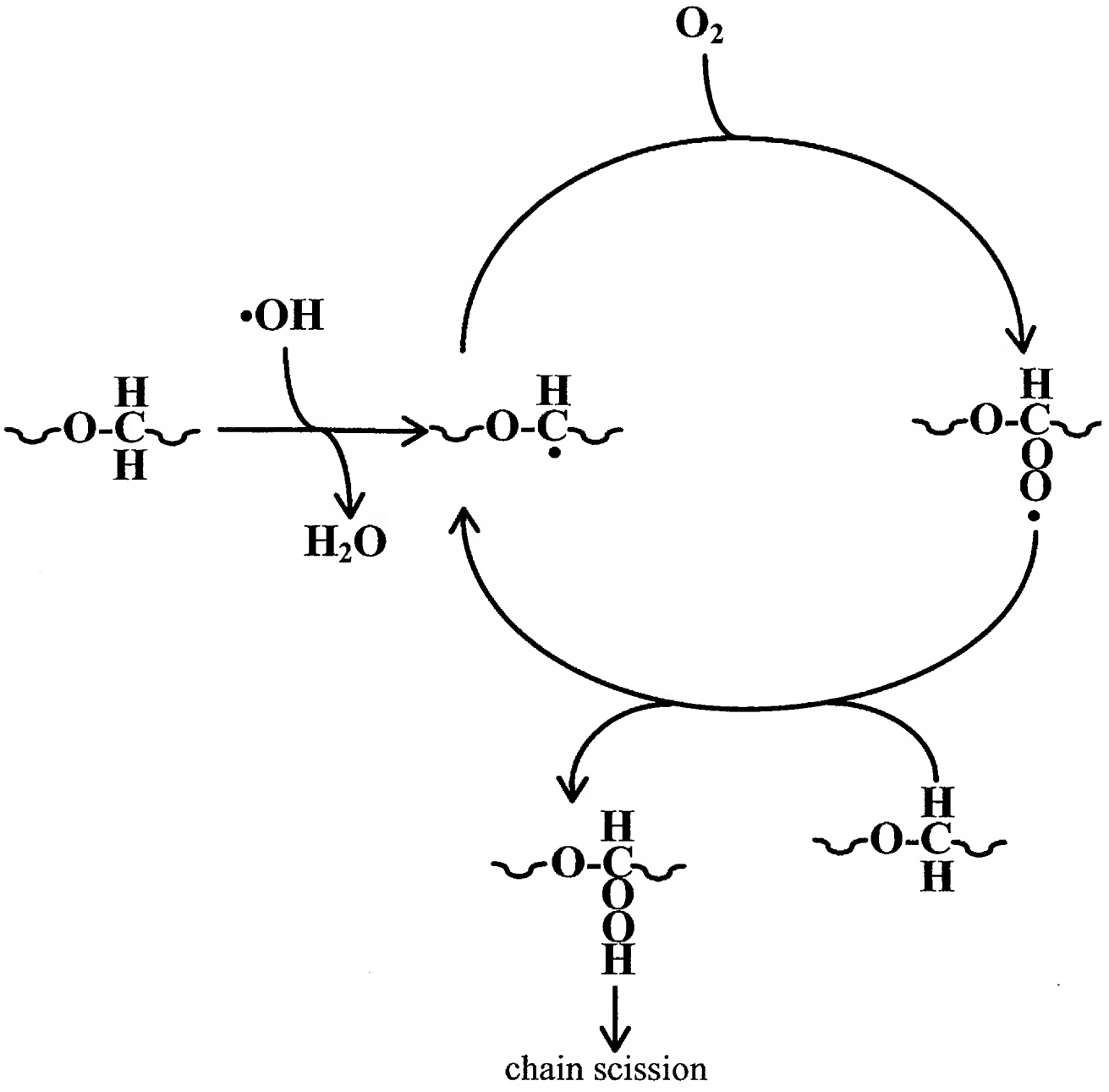

Figure 8. Proposed auto-oxidation mechanism for α-methylene of polyether.

reacts quickly to create a more stable peroxide radical. When the stable peroxide radical abstracts a hydrogen atom from another ether methylene, a hydroperoxide group is created which leads to chain scission and another polymer radical is formed. As the concentration of peroxide radicals increases the oxidation process eventually becomes autocatalytic.[10] Termination of the chain reaction occurs by radical–radical combination. When the oxygen concentration is low (below 100 mm Hg partial pressure) termination takes place almost exclusively between polymeric alkyl radicals to produce a crosslink.[10] The solubility of oxygen in the *in vitro* treatment solution is assumed to be approximately 0.01 ml/ml · atm (8 mm Hg partial pressure), and therefore termination of the PEUU auto-oxidation is thought to occur by combination of polymer radicals generating crosslinks. This would confirm a previous hypothesis that crosslinking and chain scission both occur during PEUU biodegradation.[3]

Many studies[9–11] have shown that the rate of oxidation for polymers in the solid state is controlled by the diffusion of oxygen into the polymer. To test the hypothesis that diffusion of oxygen into PEUU determines the surface specificity of degradation, the relationship of oxygen diffusion to the depth of degradation was modeled following previous approaches. In

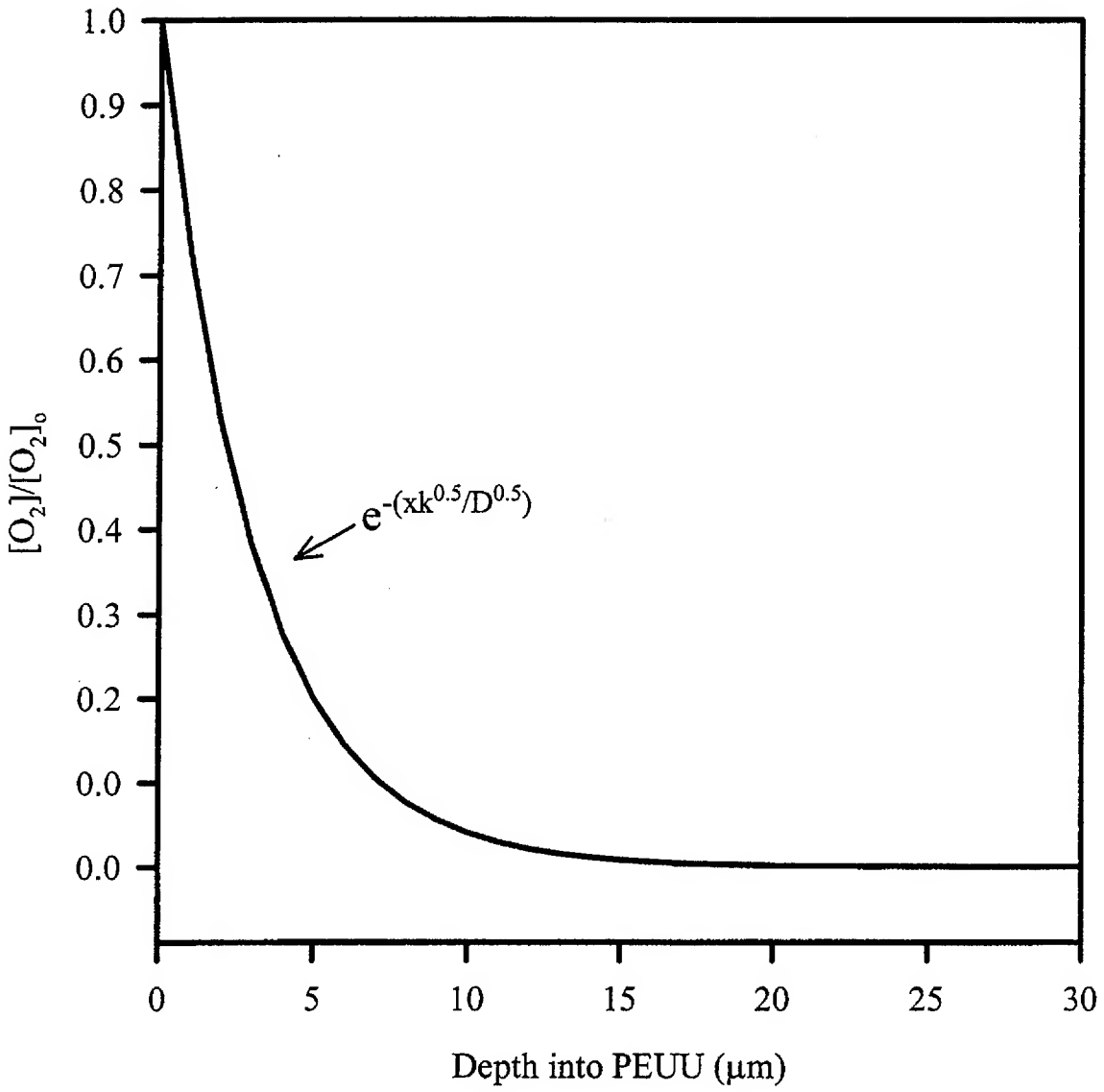

Figure 9. Normalized concentration profile of oxygen in PEUU at steady state, where $k = 0.035\ s^{-1}$ and $D = 3.4 \times 10^{-9}\ cm^2/s$.

this diffusion-reaction model, the net flux of oxygen into the PEUU is determined by the diffusion rate less the rate of consumption by reaction with polymer radicals. Assuming Fickian diffusion of oxygen with a constant diffusion coefficient, D, and a reaction rate r_{O_2}, the mass balance is described by

$$\frac{\partial[O_2]}{\partial t} = D\frac{\partial^2[O_2]}{\partial x^2} - r_{O_2} \tag{8}$$

where x is the depth from the surface into a semi-infinite PEUU solid.[22,23] This analysis also assumes that polymeric alkyl radicals are in excess to oxygen at all depths.[11] For this assumption to be valid, the initiating species (hydroxyl and hydroperoxy radicals) must transfer into the PEUU more rapidly than oxygen.

It is assumed that oxygen is consumed by an irreversible first order reaction where k_e is an effective rate constant[23]:

$$r_{O_2} = k_e[O_2] \tag{9}$$

This is valid only when the oxygen concentration is below 0.13 ml/ml · atm (100 mm Hg partial pressure).[10] Based on the arguments above, the oxygen concentration in the *in vitro* treatment solution meets this condition. At steady state, the solution to Equation (8) is given by[22]:

$$\frac{[O_2]}{[O_2]_O} = exp\left(-x\sqrt{\frac{k_e}{D}}\right). \tag{10}$$

The effective rate constant k_e includes terms for initiation, propagation, and termination. It has been shown that at low oxygen concentration and steady state, the rate of oxygen consumption in the auto-oxidation of

TABLE I
Molecular Weight of PEUU from Gel Permeation Chromatography

	M_p	M_n	M_w	PDI
Untreated	40,000	37,000	75,000	2.0
12 days *in vitro*	37,000	38,000	103,000	2.7
6 days *in vitro*+ 6 days air	15,000	19,000	51,000	2.6

M_p = peak molecular weight; PDI = M_w/M_n; average, $n = 2$.

polymers is

$$r_{O_2} = k_p[O_2]\sqrt{\frac{r_i}{k_t}} \tag{11}$$

where k_p is the rate constant for propagation, r_i is the rate of initiation, and k_t is the rate constant for termination. By substitution,

$$k_e = k_p\sqrt{\frac{r_i}{k_t}}. \tag{12}$$

Disregarding the individual rates of initiation, propagation, and termination, the overall rate of oxidation was obtained from the rate of decrease of the ether 1110 cm^{-1} ATR-FTIR absorbance. It is assumed that ether loss occurs only by the auto-oxidation mechanism, and therefore, one oxygen molecule is consumed for each ether linkage destroyed:

$$\frac{\partial\left(\frac{[C-O-C]}{[C-O-C]_O}\right)}{\partial t} = r_{O_2} \tag{13}$$

The assumption that the rate of ether oxidation is equal to the rate of oxygen consumption is commonly made to measure oxidation rates.[10] The rate of ether oxidation was determined at the surface where the oxygen concentration is constant and equal to the concentration in solution. It is assumed that because the depth of PEUU degradation is on the order of 10 μm and ATR-FTIR measured only to a depth of approximately 0.1 μm, the measured rate of ether oxidation was the rate at the surface.

The concentration of ether linkages in PEUU was determined from the stoichiometry to be 10 *M*.[12] A similar value for the ether concentration in the upper 100 Å of the PEUU was obtained by x-ray photoelectron spectroscopy.[3] The linear decrease in the ATR-FTIR ether absorbance during the initial 4 days of treatment gave a rate of ether degradation of 1.36×10^{-5} *M*/s. Assuming an oxygen concentration of 0.01 ml/ml · atm (3.9×10^{-4} *M*), the effective overall rate constant, k_e, for PEUU oxidation *in vitro* was calculated to be 0.035 s^{-1} from Equation (9).

To use Equation (10), in addition to the effective rate constant, k_e, the diffusion coefficient of oxygen in PEUU is required. Table II displays the permeability, solubility, and diffusion coefficient for oxygen in

TABLE II
Oxygen Permeability and Diffusion Values

	P × 10^{13} (cc cm/ cm^2Pa s)	D × 10^9 (cm^2/s)	S × 10^5 (cc/cc Pa)	Temperature (°C)
PEUU	0.46 ± 0.04	3.4 ± 0.3	1.4 ± 0.2*	37
LDPE[24]	2.2	460	.047	5–60
Butyl rubber[25]	0.98	8.1	1.2	25–50

*Calculated.

PEUU, and for comparison, the values for low-density polyethylene[24] and butyl rubber.[25] The diffusion coefficient of oxygen in PEUU at 37°C and 90% relative humidity is 3.4×10^{-9} cm^2/s, which is similar to that in another elastomer, butyl rubber (8.1×10^{-9} cm^2/s).

Using these values for k_e and *D*, the concentration of oxygen versus depth into the PEUU was obtained from Equation (10). This analysis (Fig. 9) shows that at steady state the reaction of diffusing oxygen is sufficiently rapid that molecular oxygen penetrates only to a depth of 10–15 μm. As a result, PEUU degradation is confined to this depth. Previously, this diffusion-reaction concept successfully modeled a 1-mm depth of oxidation for artificially weathered low density polyethylene (LDPE).[11] The depth of the oxidized layer is determined by the ratio k_e/D in Equation (10). The larger depth of the LDPE-oxidized layer compared to PEUU reflected a much lower value of k_e/D (5.7 cm^2 for LDPE and 10^7 cm^2 for PEUU). Both a higher diffusion coefficient for oxygen in LDPE (460×10^{-9} cm^2/s) and a smaller rate constant for oxidation were responsible for the smaller k_e/D of LDPE.

The preceding analysis of *in vitro* oxidation has implications for the *in vivo* degradation of PEUU. As reported previously, the *in vitro* system mimics many features of biodegradation. Specifically, implanted PEUU that is not stabilized by antioxidants exhibits an oxidized surface layer of about the same depth, 10 μm, as the PEUU treated *in vitro*.[6] This suggests that the diffusion-reaction model is also applicable to *in vivo* oxidation. It has been proposed that hydroxyl and hydroperoxy radicals, available at the interface of adherent leukocytes with the PEUU, are responsible for *in vivo* oxidation.[6] It appears that the local concentration of these radicals is high enough to sustain auto-oxidation of the PEUU using oxygen from the extracellular fluid and/or from nonradical products of the leukocyte respiratory burst.[16]

CONCLUSIONS

This work demonstrates that PEUU degradation is a surface phenomenon resulting from a classical auto-oxidation mechanism. By modeling the depth of the

surface degraded layer with a diffusion-reaction model, it is shown that PEUU degradation is controlled by diffusion of oxygen into the polymer. Correspondence between the calculated depth (10–15 μm) and the depth of the degraded layer determined for PEUU treated *in vitro* and *in vivo* suggests that biodegradation of implanted PEUU at the cell–polymer interface is sustained by an auto-oxidation mechanism. Although the chemical reaction is confined to a surface layer, the physical effects may be more profound. If the PEUU is strained, the brittle, degraded layer can pit and crack. With time, the cracks can propagate into the bulk of the PEUU, leading to failure of the film or coating.

The authors extend appreciation to Professor Charles Rogers and Dr. Eugene Stepanov for their helpful discussions, and to the National Institutes of Health (Grant HL-25239) for their generous financial support.

References

1. D. J. Parins, K. M. Black, K. D. McCoy, and N. J. Horvath, *In Vivo Degradation of a Polyurethane,* Cardiac Pacemakers, Inc., St. Paul, Minnesota, 1981.
2. Q. Zhao, J. Casas-Bejar, P. Urbanski, and K. Stokes, "Glass wool–H_2O_2/$CoCl_2$ test system for *in vitro* evaluation of biodegradative stress cracking in polyurethane elastomers," *J. Biomed. Mater. Res.*, **29,** 467–475 (1995).
3. M. A. Schubert, M. J. Wiggins, M. P. Schaefer, A. Hiltner, and J. M. Anderson, "Oxidative biodegradation mechanisms of biaxially strained poly(etherurethane urea) elastomers," *J. Biomed. Mater. Res.*, **29,** 337–347 (1995).
4. M. Szycher, "Biostability of polyurethane elastomers: A critical review," *J. Biomed. Appl.*, **3,** 297–401 (1988).
5. Q. Zhao, A. K. McNally, K. R. Rubin, M. Reiner, Y. Wu, V. Rosa-Caprara, J. M. Anderson, A. Hiltner, P. Urbanski, and K. Stokes, "Human plasma α_2-macroglobulin promotes *in vitro* oxidative stress cracking of Pellethane 2363-80A: *In vivo* and *in vitro* correlations," *J. Biomed. Mater. Res.*, **27,** 379–389 (1993).
6. Y. Wu, C. Sellitti, J. M. Anderson, A. Hiltner, G. A. Lodoen, and C. R. Payet, "An FTIR-ATR investigation of *in vivo* poly(etherurethane) degradation," *J. Appl. Polym. Sci.*, **46,** 201–211 (1992).
7. K. Stokes, P. Urbanski, and J. Upton, "The *in vivo* autoxidation of polyether polyurethane by metal ions," *J. Biomater. Sci. Polymer Edn.*, **1,** 207–230 (1990).
8. Q. Zhao, N. Topham, J. M. Anderson, A. Hiltner, G. Lodoen, and C. R. Payet, "Foreign-body giant cells and polyurethane biostability: *In vivo* correlation of cell adhesion and surface cracking," *J. Biomed. Mater. Res.*, **25,** 177–183 (1991).
9. A. Popov, N. Rapoport, and G. Zaikov, *Oxidation of Stressed Polymers,* Gordon and Breach Science Publishers, New York, 1991.
10. B. Ranby and J. F. Rabek, *Photodegradation, Photooxidation and Photostabilization of Polymers,* Wiley-Interscience, New York, 1975.
11. A. V. Cunliffe and A. Davis, "Photo-oxidation of thick polymer samples—part II: The influence of oxygen diffusion on the natural and artificial weathering of polyolefins," *Polymer Deg. Stabil.*, **4,** 17–37 (1982).
12. M. Renier, Y. K. Wu, J. M. Anderson, A. Hiltner, G. A. Lodoen, and C. R. Payet, "Characterization of extractable species from poly(etherurethane urea) (PEUU) elastomers," *J. Biomater. Sci. Polym. Edn.*, **5,** 511–529 (1994).
13. K. Imada, H. Takokoro, A. Umehara, and S. Murahashi, "Normal vibrations of the polymer molecules of helical conformation. VI. Polytetrahydrofuran and deuterated polytetrahydrofurans," *J. Chem. Phys.*, **42,** 2807–2816 (1965).
14. Y. K. Wu, G. A. Lodoen, J. M. Anderson, E. Baer, and A. Hiltner, "Creep of a poly(etherurethane urea) in an oxidative environment," *J. Biomed. Mater. Res.*, **28,** 515–522 (1994).
15. J. O. Edwards and R. Curci, "Fenton type activation and chemistry of hydroxyl radical," in *Catalytic Oxidations with Hydrogen Peroxide as Oxidant,* G. Strukul (ed.), Kluwer Academic Publishers, Dordrecht, 1992, pp. 97–152.
16. B. Halliwell, "Oxygen radicals: A common sense look at their nature and medical importance," *Med. Biol.*, **62,** 71–77 (1984).
17. J. K. Klaning, E. Larsen, and K. Sehested, "Oxygen atom exchange in aqueous solution by $O^- + H_2O \rightarrow OH^- + OH$ and $OH + H_2O \rightarrow H_2O + OH$. A study of hydrogen atom transfer," *J. Phys. Chem.*, **98,** 8946–8951 (1994).
18. D. W. Arnold, X. Cangshan, and D. M. Neumark, "Spectroscopy of the transition state: Elementary reactions of the hydroxyl radical studied by photoelectron spectroscopy of $O^-(H_2O)$ and $H_3O_2^-$," *J. Chem. Phys.*, **102,** 6088–6099 (1995).
19. Y. Ogata, K. Tomizawa, and K. Furuta, "Photochemistry and radiation chemistry of peroxide," in *The Chemistry of Peroxides,* S. Patai (ed.), Wiley, Chichester, 1983, pp. 711–776.
20. E. B. Abuin, E. A. Lissi, and L. Avaria, "Effect of pH on the behavior of hydrogen peroxide as an inhibitor or chain transfer agent," *J. Polym. Sci. Polym. Lett.*, **26,** 501–503 (1988).
21. W. Lang and R. Zander, "Salting-out of oxygen from aqueous electrolyte solutions: Prediction and measurement," *Ind. Eng. Chem. Fundam.*, **25,** 775–782 (1986).
22. J. Crank, *The Mathematics of Diffusion,* 2nd ed., Oxford University Press, Oxford, 1975, pp. 326–351.
23. D. A. Frank-Kamenetskii, *Diffusion and Heat Exchange in Chemical Kinetics,* University Press, Princeton, New Jersey, 1955, pp. 46–127.
24. S. Pauly, ed., *Polymer Handbook,* Wiley, New York, 1989, pp. 435–450.
25. J. Y. Moisan, "Effects of oxygen permeation and stabilizer migration on polymer degradation," in *Polymer Permeability,* J. Comyn (ed.), Elsevier Applied Science, London, 1985, p. 127.

Received February 23, 1996
Accepted April 22, 1996

Exhibit B

Journal of Biomaterials Applications
http://jba.sagepub.com

Polyurethane Elastomer Biostability

Ken Stokes, Rick McVenes and James M. Anderson

J Biomater Appl 1995; 9; 321
DOI: 10.1177/088532829500900402

The online version of this article can be found at:
http://jba.sagepub.com/cgi/content/abstract/9/4/321

Published by:
SAGE Publications
http://www.sagepublications.com

Polyurethane Elastomer Biostability

KEN STOKES* AND RICK MCVENES
Medtronic, Inc.
7000 Central Avenue NE
Minneapolis, MN 55432-3576

JAMES M. ANDERSON
University Hospitals of Cleveland
The Institute of Pathology of Case Western Reserve University
2085 Adelbert Road
Cleveland, OH 44106-2622

ABSTRACT: Polyurethanes have unique mechanical and biologic properties that make them ideal for many implantable devices. They are subject to some *in vivo* degradation mechanisms, however. Polyester polyurethanes are subject to hydrolytic degradation and are no longer used in long-term implanted devices. Polyether polyurethanes, while hydrolytically stable, are subject to oxidative degradation in several forms, including environmental stress cracking and metal ion oxidation. Mineralization is also known to occur. A new polycarbonate polyurethane has superior biostability in early *in vivo* qualification tests compared to the polyether polyurethanes, including no evidence of hydrolysis, ESC or MIO.

INTRODUCTION

The word "polyurethane" can be applied to a huge number of different compositions with surprisingly varied applications. This paper is concerned with one subset of the polyurethane family of materials

*Author to whom correspondence should be addressed.

0885-3282/95/04 0321-034 $10.00/0

which has enormous utility and potential in the implantable biomedical device field. These are the polyurethane elastomers and engineering thermoplastics. Generally speaking, those used in medical devices are block copolymers consisting of aromatic or aliphatic polyurethane "hard segments" and aliphatic polyester or polyether "soft segments." These polymers have unmatched combinations of physical, chemical, electrical and biological properties. As a general rule, they offer high tensile strength and elongation, high tear strength, excellent wear resistance, and superior biocompatibility (including blood compatibility). They are excellent electrical insulators. Depending on the ratio of hard to soft segments and the molecular weight of the segments, one can vary the hardness, lubricity, flexibility (elastic modulus) and many other properties. Thus, polyurethane elastomers have been extensively evaluated for use as artificial heart diaphragms, heart valves, joint prostheses, vascular grafts, urethral catheters, mammary prostheses, penile prostheses, and many other devices intended for long-term implant. The polyester polyurethanes were used until only recently as coverings for breast prostheses. Polyether polyurethane elastomers have been used as insulation for neurologic leads since 1975 and cardiac leads since 1977. Rigid polyether polyurethane is used in connector modules for implantable cardiac pacemakers, defibrillators and neurologic stimulators.

While the use of polyurethanes elastomers in medical devices has contributed greatly to an improved quality of life for many patients, the full promise of these materials has yet to be fulfilled. The (aliphatic) polyester polyurethanes are subject to hydrolytic degradation, therefore, they are no longer used in long-term implantable devices. The softer grades of polyether polyurethanes used in implanted electrostimulators are subject to stress cracking and autoxidative phenomena, whereas the hardest grades are inherently more stable. Controversy developed in the pacing industry based on higher than expected failure rates in some devices and excellent durability in others. In spite of the fact that manufacturers appear to have learned how to make implantable polyurethane insulated leads with acceptable to excellent longevity, the litigious environment in the United States has driven some polymer suppliers to make their materials unavailable for implantable devices in the near future [1]. As we move into the mid 1990s, therefore, the biomedical device industry is faced with the need to find replacement polymers in addition to the ever present desire to develop improved materials and devices. Promising new elastomers based on polycarbonate polyurethane chemistry are in the process of being qualified for long-term implantable use.

POLYURETHANE CHEMISTRY AND PHYSICS

Polyurethane Elastomer Chemistry

The term "urethane" refers to the carbamate linkage as shown in Equation (1). In polymers, this is typically made by the addition of an isocyanate to a hydroxyl where

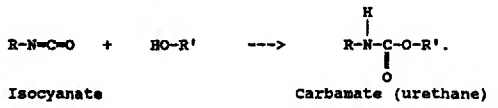

(1)

Polymers composed only of isocyanate and alcohol reaction products, however, are not usually used in implantable biomedical devices. The elastomers used in implantable devices are typically block copolymers based largely on other chemistries, such as polyester or polyether, linked together by urethane or urethane and urea segments. They are usually the addition products of relatively high molecular weight polyester or polyether diols with an excess of diisocyanate. The polymer is then "chain extended" by the addition of a short chain diol or diamine to the desired stoichiometry. Alternatively, some polymers are made continuously with a twin screw extruder. The mixed soft segment and chain extender can be metered into one side and the isocyanate metered into the other side, or an isocyanate/chain extender adduct can be used with the soft segment diol. The end groups can be hydroxyl or isocyanate, depending on the stoichiometry, or the polymer can be "end capped" with a reactive monofunctional molecule. If the polymer is isocyanate terminated, then the end groups in the finished polymer can react with urethane linkages or, in some cases, urea groups in the main chain to form crosslinks as shown in Equations (2) and (3).

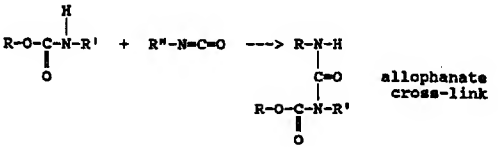

(2)

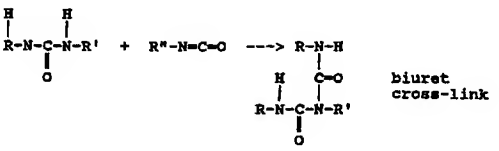

(3)

Such allophanate or biuret crosslinks are thermally labile at tempera-

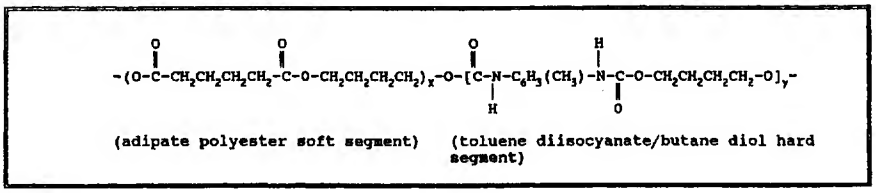

Figure 1. Typical aromatic polyester (adipate) polyurethane hard and soft segments.

tures below those used for thermal processing. During extrusion, the isocyanate end group is reformed. Because it is nearly impossible to completely and absolutely dry the polymer before extrusion or molding, the freed isocyanate end groups will preferentially scavenge any residual moisture to form amine end groups and a trace of CO_2. Thus, isocyanate terminated polymers are typically crosslinked and insoluble prior to thermal processing, but can be dissolved in appropriate solvents after extrusion or molding.

Of course, there are many possible soft segment diols, isocyanates and chain extenders that could be used. The most common polyester polyurethane elastomers are made with an adipate soft segment and a toluene diisocyanate/butane diol hard segment as shown in Figure 1. All polyether polyurethanes used in implantable devices use polytetramethylene oxide diol (PTMO) as the soft segment (Figures 2–4). The hard segments are made either with methylene bis phenyl diisocyanate (diphenyl methane diisocyanate, MDI, Figures 2 and 3) or methylene bis cyclohexane diisocyanate (CHDI, Figure 4). Some polyether polyurethanes use 1,4 butane diol (BD) as a chain extender (Figures 2 and 4), others use aliphatic diamines (Figure 3). The newest polyurethane elastomers substitute a polycarbonate soft segment for the PTMO, as shown in Figures 5 and 6.

At present, only polyether polyurethanes are used in implantable devices. These are either the Pellethane 2363® series of thermoplastics (Figure 2), or polymers similar to Biomer® (Figure 3). The Pellethane 2363 series has a PTMO soft segment with MDI/BD hard segments. It is offered in various Shore hardness and end group categories. The isocyanate terminated polymers have designations ending in A, while the hydroxyl terminated polymers end in AE. The very flexible Shore 80 polymer has the highest molecular weight PTMO diol, whereas the more rigid 75D material has the shortest. Most cardiac pacing leads

Pellethane 2363® is a registered trademark of The Dow Chemical Co.
Biomer® is a registered trademark of Ethicon, Inc.

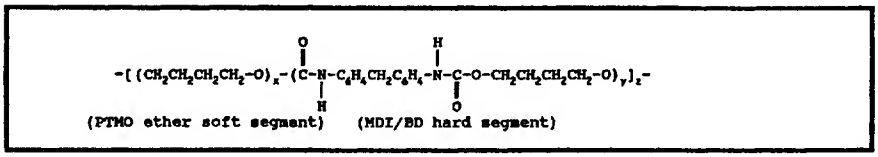

Figure 2. Typical aromatic polyether polyurethane hard and soft segments.

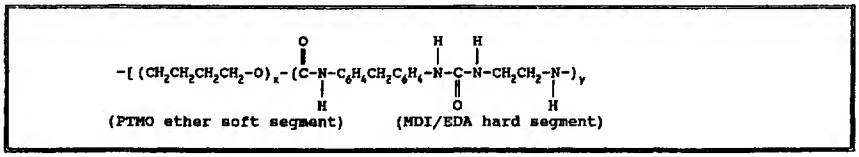

Figure 3. Typical aromatic polyether polyurethane-urea hard and soft segments.

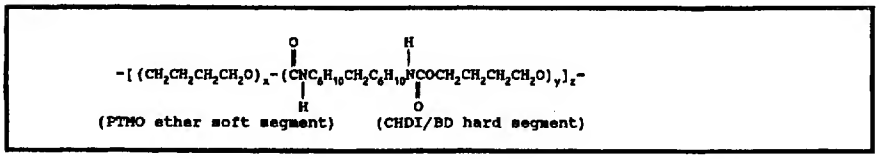

Figure 4. Typical aliphatic polyether polyurethane hard and soft segments.

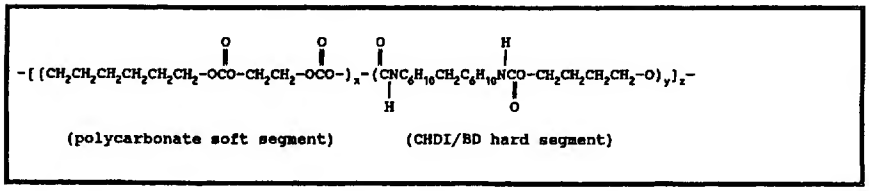

Figure 5. Typical aliphatic polycarbonate polyurethane hard and soft segments.

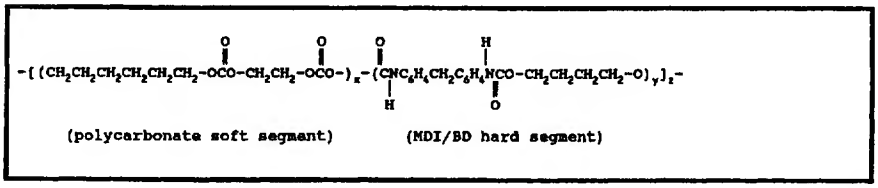

Figure 6. Typical aromatic polycarbonate polyurethane hard and soft segments.

have been insulated with extruded Pellethane 2363-80A or 55D, although some have been made with Pellethane 2363-90A. Many implantable pulse generator connectors are made of injection molded Pellethane 2363-75D.

A relatively small number of cardiac pacing leads are insulated with a Biomer-like polymer, Surethane® (Figure 3). Structurally, this is similar to Pellethane 2363-80A, but the 1,4 butane diol chain extender is replaced with a diamine. This polyether polyurethane-urea cannot be reliably converted by conventional thermoplastic processes because the urea functionality decomposes at temperatures below those required for extrusion and injection molding. Thus, it must be applied from solvent.

Several other polyether polyurethanes have been evaluated for use in implantable devices, but so far have found utility primarily in devices intended for temporary use. Tecoflex® (Figure 4) is a series of polymers similar to the Pellethanes, except that a cycloaliphatic diisocyanate (CHDI) has been substituted for the MDI [2]. Tecothane® is reportedly structurally similar to Pellethane 2363 (Figure 2) [3].

The newest polyurethanes substitute a polycarbonate soft segment for PTMO. ChronoFlex AL® has a cycloaliphatic (CHDI/BD) hard segment with hydroxyl end groups (Figure 5) [4]. ChronoFlex AR® is a polycarbonate analogue of Biomer with an MDI/BD hard segment. Corethane® uses the same soft segment with an aromatic MDI/BD hard segment (Figure 6) [5].

Polyurethane Elastomer (Molecular) Physics

The polyurethane elastomers derive their unique physical properties from their segmented structure and the relatively easy formation of significant hydrogen bonding in their hard segments. Immediately upon cooling from the melt, or evaporation of solvent, the polymer is relatively amorphous and phase mixed. With time, the hard and soft segments separate into separate phases, like oil in water (Figure 7) [6]. The soft segments are usually thought to remain amorphous, but the hard segments tend to crystallize as shown in Figure 8. The phase-separated hard segments then act like reinforcing fillers for the more

---

Surethane® is a registered trademark of Cardiac Control Systems, Inc.
Tecoflex® is a registered trademark of Thermedics, Inc.
Tecothane® is a registered trademark of Thermedics, Inc.
ChronoFlex AL® is a registered trademark of PolyMedica, Inc.
ChronoFlex AR® is a registered trademark of PolyMedica, Inc.
Corethane® is a registered trademark of Corvita, Inc.

Figure 7. Schematic hard and soft segment domain structure. Reprinted from Bonart [6].

amorphous soft segments in a micro domain structure such as that shown in Figure 7. Annealing can increase the degree of phase separation and crystallization.

The polyurethane elastomer's phase separation with hydrogen bonded crystallinity in the hard segment produces the unique properties of this class of materials. Mechanical properties change with time just after processing as phase separation occurs. Thus, it is critical, perhaps more so than with other classes of polymers, to allow adequate conditioning time before property measurements are made. Once equilibrated, tensile strength typically is in the 6000 to 8000 psi range with ultimate elongations from 400 (harder polymers) to 700% (softer

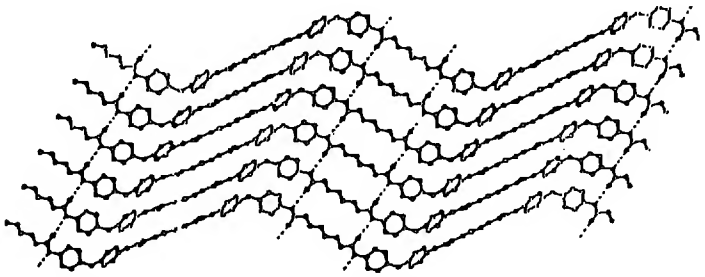

Figure 8. β-Pleated conformation of phase separated, crystalline aromatic polyurethane hard segments, Reprinted from Bonart [6].

polymers). The die C tear strength is typically in the 400 to 600 pli range. Elastic moduli range from very flexible to rigid. In comparison, the typical "MDX" silicone rubber has about 1000 psi tensile strength with about 350% elongation and about 70 pli tear strength. The ETR (enhanced tear resistant or "tough") silicone rubbers typically have significantly higher elongations and tear strengths of $\geq$200 pli.

While the polyurethane elastomers have excellent mechanical and biological properties for use in implanted devices, their utility extends only as far as their biostability allows.

THE BIOLOGIC ENVIRONMENT AND BIOSTABILITY

The mammalian body is an incredibly harsh environment for a foreign material and an implanted device. While much has been learned about the implant environment, there is *much* more that remains to be learned. Polyester polyurethanes were investigated extensively for use in the artificial heart, until their susceptibility to hydrolytic degradation was recognized [7,8]. The polyether polyurethanes were believed to be the answer, since they are hydrolytically stable under most *in vivo* conditions. Long-term premarket biostability testing was done on two Pellethanes and Biomer [9–13]. It was not until Pellethane was used in marketed devices that several previously unknown oxidative failure mechanisms were discovered that affect the polyether soft segment [14]. To overcome this susceptibility to oxidative failure, polycarbonate polyurethanes have been suggested to provide both hydrolytic and oxidative biostability. Before their biostability can be addressed, however, the *in vivo* environment and the biodegradation mechanisms affecting their polyester and polyether precursors will be reviewed.

The Humoral Environment

The intracellular and extracellular fluids (interstitial fluids, blood plasma, cerebrospinal fluid, intraocular fluid, etc.) constitute the humoral environment [15]. The total amount of water in an average (70 kg) man is about 40 liters, or an average of 57% of the body weight. Water is, of course, the primary agent for hydrolytic degradation. Other components of the humoral environment may vary, but in general include electrolytes (primarily Na^+, K^+, Ca^{++}, Mg^{++}, Cl^-, $HPO_4^=$, $SO_4^=$, HCO_3^-), proteins and nonelectrolytes such as phospholipids, cholesterol, neutral fat, glucose, urea, lactic acid, uric acid, creatinine, bilirubin, bile salts, and many more.

Polyurethane Hydrolysis

The aliphatic ester linkages in polyester polyurethanes are susceptible to hydrolytic degradation where [16],

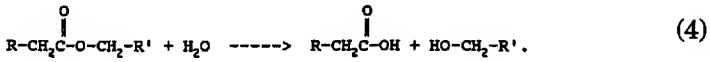

(4)

The unique toughness, flexibility, and blood compatibility of polyester polyurethanes made them ideal candidates for blood pump diaphragms and other implantable devices until their susceptibility to hydrolysis was recognized. Their use in plastic and reconstructive surgery initially appeared promising with minimal acute inflammation. Thin fibrous capsules formed with good fixation due to ingrowth into pores. However, they degraded and became fragmented within months as a result of hydrolytic decomposition. In spite of this, many plastic surgeons preferred to use breast implants with a thin coating of polyester polyurethane foam. Today there is considerable controversy over the biocompatibility of the degrading polymer [17–19].

The urethane linkage is not considered to be susceptible to hydrolysis under ordinary physiologic circumstances. At elevated temperatures, such as are encountered in extrusion or injection molding, damp polymer can hydrolyze if not thoroughly dried.

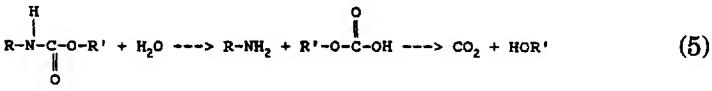

(5)

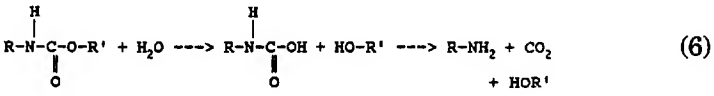

(6)

Thus, while aliphatic ester-free polyurethanes are considered to be hydrolytically stable after they are implanted, degradation can be initiated during the manufacturing process which can result in physical defects (such as bubbles) and reduction in physical properties. The formation of bubbles, even if microscopic, may be of significance, especially with regard to mineralization [20]. It is, therefore, critically important that the resin be thoroughly dried, preferably to $<0.1\%$ water by weight, prior to extrusion or molding. The same is true of solvent-based applications or analytical techniques, including molecular weight determinations.

The *in vivo* Oxidative Environment

With rare exceptions, such as nonthrombogenic surfaces in blood contact, implanted devices do not interface directly with the tissues they were designed for. In most cases, the actual chronic tissue interface is (from the device "out") the biomaterial surface, a layer or layers of foreign body giant cells and/or macrophages, then a fibrotic capsule composed primarily of collagen containing phagocytic cells and fibroblasts and finally, the native tissue [21]. The cellular component of the foreign body reaction can have a major effect on an implanted material's biostability [22]. When activated, these cells can release numerous enzymes and oxidants, some of which are considered to be of significance for the biostability of an implanted material [22]. Perhaps the most important appear to be the oxidants (H_2O_2, O_2^-, $HO^\cdot$) and hydrolytic enzymes [21–29]. The details of the foreign body response to implanted devices have been covered elsewhere [21,22]. Even devices implanted in tissues with very low oxygen tension can be exposed to significant amounts of highly reactive oxidants as a result of the ubiquitous foreign body response. Compared to the worldly environment, the oxygen tension in the venous system and most other tissues is very low. Thus, at first one might think that autoxidation at clinically significant rates is not favored in these tissues. However, inflammation and the foreign body response result in the release of oxidants (including H_2O_2, O_2^- and $^\cdot OH$) directly on the surface of the device. These can interact with themselves, the polymer (and other device components) and the autoxidation kinetic chain in various ways including [30]:

$$HO^* + H_2O_2 \longrightarrow H_2O + {}^*OOH \quad (7)$$

$$M^{n*} + {}^*OOH \longrightarrow (M\text{-}OOH)_{complex} \quad (8)$$

$$HOO^* + H_2O_2 \longrightarrow H_2O + O_2 + {}^*OH \quad (9)$$

$$HOO^* \longrightarrow O_2^{-*} + H^+ \quad (10)$$

These free radicals have very short half lives and can be effective over only very limited distances. Thus, oxygen free radicals will have the greatest effect immediately under the cells, on the device surface [31–33]. They will initiate and propagate autoxidation from the outside of the biomaterial inward. In this case, autoxidation will be observed initially as surface defects. More stable oxidants, such as H_2O_2, may migrate into the biomaterial to decompose within the polymer or on

metallic components within the device [34]. In this case, H_2O_2 can initiate and propagate degradation from the inside of the device, outward.

Autoxidation Mechanisms of Polymers in General

Autoxidation has been defined as the thermal oxidation that takes place between room temperature and about 150°C and takes place by a typical free-radical chain reaction [30]. All organic polymers are susceptible to autoxidation to varying degrees. The rate of degradation varies dramatically as a function of the polymer's structure and the presence of catalysts. The complex autoxidation chain reaction is self propagating once started. The initiation reaction yields products that can themselves react spontaneously with polymer molecules. The major steps in the chain can be generalized, where P = polymer [35]:

Initiation

$$PH \xrightarrow{X} P^* + H^* \quad (H^* \text{ abstraction}) \text{ or} \tag{11}$$

$$PP \xrightarrow{X} P^* + P^* \quad (\text{chain cleavage}). \tag{12}$$

X can include radiation, light, heat, ultrasonics, mastication, strain, metal ions, nascent oxygen, ozone, etc. Thus, initiation typically occurs during processing operations involving heat and shear, such as pelletizing, compounding, extrusion, or injection molding. Autoxidation is usually initiated by abstraction of a hydrogen atom [Equation (11)]. When the material is under tension, however, chain cleavage [Equation (12)] can predominate. Initiation can be random or site specific. Random initiation is more probable in hydrocarbon polymers such as polyethylene or polypropylene. The rate determining step is usually hydrogen abstraction [30]. The ease of hydrogen abstraction depends on the type of CH bond present. For example, hydrogen atoms adjacent to carboxyl, carbonyl and other electron withdrawing groups are more easily abstracted by free radicals. Thus, initiation tends to be site specific in polymers such as polyamides, polyethers, and polyesters.

Hydroperoxide Formation

$$P^* + O_2 \longrightarrow POO^* \tag{13}$$

$$POO^* + PH \longrightarrow POOH + P^* \tag{14}$$

Oxygen is ubiquitous in the ordinary environment and the reaction between polymer free radicals and oxygen is extremely rapid. Thus, the concentration of peroxy free radicals is much greater than polymer free radicals and polymer hydroperoxides are ubiquitous. On the other hand, the concentration of hydroperoxides in polymers is usually so low that they are not detectable by ordinary analytical techniques. Even at very low concentrations, they can be of significant importance in subsequent degradation reactions.

Propagation

Propagation of the chain reaction usually begins with degradation of the hydroperoxide groups. However, polymer hydroperoxides are typically resonance stabilized so that they can exist for substantial periods of time without degrading. They are relatively easily decomposed by catalysts (Y) such as light, heat, free radicals, or metal ions.

$$POOH \xrightarrow{Y} PO^{*} + {}^{*}OH \quad (42\ Kcal/mole) \tag{15}$$

$$POOH \xrightarrow{Y} P^{*} + {}^{*}OOH \quad (70\ Kcal/mole) \tag{16}$$

$$POOH \xrightarrow{Y} POO^{*} + {}^{*}H \quad (90\ Kcal/mole) \tag{17}$$

Under ordinary conditions, the low dissociation energy favors Equation (15), although it is difficult to say what constitutes "ordinary" in implanted devices. Typical degradation products include carbonyl and hydroxyl groups. The reaction can take many paths which, depending on the conditions, can have few or many steps. The number of propagation steps started by a single initiation reaction is defined as the kinetic chain length. A few of the more straightforward possible steps in the kinetic chain include:

$$PO^{*} + {}'PH \longrightarrow POH + {}'P^{*} \tag{18}$$

$$POO^{*} + {}'PH \longrightarrow POOH + {}'P^{*} \tag{19}$$

$$POOH + {}'PO^{*} \longrightarrow PCO^{*} + {}'POOH \tag{20}$$

$$POOH + HO^{*} \longrightarrow POO^{*} + H_2O \tag{21}$$

Termination

Eventually, termination reactions occur to produce nonreactive products. If the oxygen partial pressure is low (<100 mm Hg), then

$$POO^{\bullet} + P' \longrightarrow POOP' \quad (22)$$

$$P^{\bullet} + {}^{\bullet}P' \longrightarrow PP' \quad (23)$$

$$PO^{\bullet} + {}^{\bullet}P' \longrightarrow POP' \quad (24)$$

Under these conditions, the reaction is not well sustained due to a lack of oxygen and it has a relatively short kinetic chain length. If the oxygen partial pressure is relatively high ($\geq$200 mg Hg), then the predominating terminating reactions include:

$$2POO^{\bullet} \longrightarrow POOP + O_2 \quad (25)$$

Thus, oxygen needed to sustain the reaction can be regenerated, extending the kinetic chain length.

Metal Ion Oxidation (MIO)

Implanted polyether polyurethane devices which contain metallic components may be subject to bulk oxidation catalyzed by corrosion products. This mechanism, called metal ion oxidation (MIO) was discovered and characterized in implanted polyether polyurethane insulated cardiac pacing leads [14]. The metal alloy conductors inside the lead have no effect on the polymer under laboratory ambient conditions. Neither does H_2O_2. The presence of H_2O_2 *and* the metal alloys, however, can produce a synergistic acceleration of autoxidation *in vitro*. Some of the reactions that can be specific to MIO (in addition to the above autoxidation mechanism per se) are as follows:

$$M^{n+} + H_2O_2 \longrightarrow HO\text{-}O^{-}H^{\bullet} + M^{(n+1)+} \quad (26)$$

$$M^{n+} + HO^{\bullet} \longrightarrow HO^{-} + M^{(n+1)+} \quad (27)$$

$$M^{n+} + O_2 \longrightarrow M^{(n+1)+} + O_2^{\bullet-} \quad (28)$$

$$O_2^{\bullet-} + H^{+} \longrightarrow HOO^{\bullet} \quad (29)$$

$$O_2^{\bullet-} + PH \longrightarrow PO^{\bullet} + HO^{-} \quad (30)$$

$$M^{n+}\ O_2 \longrightarrow (M\text{-}O_2)_{complex} \quad (31)$$

$$(M^{n+}O_2)_{complex} + M^{n+}(XH) \longrightarrow M^{(n+1)+}X^{-} + HOO^{\bullet} + M^{n+} \quad (32)$$

(where X can be, but is not limited to polymer)

$$\begin{array}{ccc} M^{n+} + O_2 & \text{<-----> } & M^{(n+1)+} + O_2^{\bullet} \\ \downarrow\uparrow & & \downarrow PH \\ M^{n+}O_2\bullet & \xrightarrow{PH} & HOO\bullet + P\bullet + M^{n+} \end{array} \quad (33)$$

In several of the above equations, metal is oxidized. This has significance because transition metals can initiate polymer oxidation directly where;

$$M^{(n+1)+} + PH \text{ -----> } P\bullet + M^{n+} + H^{+} \quad (34)$$

In addition, metal ions can also react with polymer hydroperoxides to propagate the reaction.

$$M^{(n+1)+} + POOH \text{ -----> } M^{n+} + POO\bullet + H^{+} \quad (35)$$

$$M^{n+} + POOH \text{ -----> } M^{(n+1)+} + PO\bullet + HO^{-} \quad (36)$$

Metallic corrosion products can react with some of the products of degradation. For example,

$$M^{(n+1)+} + RCH_2OH \text{ -----> } M^{n+} + RC^{\bullet}HOH + H^{+} \quad (37)$$

$$M^{(n+1)+} + RCHO \text{ -----> } M^{n+} + RC^{\bullet}=O + H^{+} \quad (38)$$

Equations (34)–(38) are of particular interest since we have recently verified that MIO can occur within cardiac pacing leads in locations where there was no fibrotic encapsulation. Therefore, no foreign body response was present; therefore, no H_2O_2 was involved. Given the extremely low oxygen tension in these tissues, it appears that MIO can occur by anaerobic processes as well as by autoxidation.

Coury et al., determined *in vitro* (in distilled water at 70 or 90°C) that the oxidation potential of an ion must be ≥ about 0.8 V to oxidize a polyether polyurethane [36]. In his studies, Co (II) (as $CoCl_2$) does not attack the polymer, having too low an oxidation potential. Co (III) does have a high enough oxidation potential, but this exceeds that required to oxidize water (E° = 1.2 V). Thus, in distilled water, simple cobalt salts do not provoke MIO. Nonetheless, based on *in vitro* tests at 37°C in 3% H_2O_2 and in real time (two years) *in vivo* studies using metals per se (not metallic salts), we have shown that the most likely catalyst for MIO in polyether polyurethane insulated leads is a cobalt species [34]. It must be kept in mind that the oxidation potentials listed in the

Handbook of Chemistry and Physics are determined in distilled water at standard temperature and pressure [37]. While the environment within a pacing lead is not well understood, it is certainly not distilled water. The oxidation potential of an ion depends on its environment and what it is dissolved in or complexed with. It is reasonable, in fact, to assume that a metal ion can complex with additives within the polymer, including the antioxidant and extrusion lubricant (a bis stearamide "wax") as well as with the polymer per se [38]. Complexation can significantly increase an ion's oxidation potential, as explained by Pauling's valence bond theory. For example, the arrangements of electrons in the 3d level for Co (II) are shown in Figure 9. As a simple ion, the 3d level has two shared pairs and three singlet electrons. When complexing occurs with octahedral coordination of the metal with cyanide, for example, the use of two of the 3d orbitals for d^2sp^3 hybridization requires that one 3d electron is promoted to the nearest vacant orbital of higher energy, which is the 5s orbital. The electron can be easily lost from this high energy level so that oxidation to the trivalent anion occurs easily. Similarly, the complexes of metallic corrosion products with electrolytes, proteins, lipids, polymers, bis stearamide wax, etc. *could* be much stronger oxidants than the base ion per se. Such complexes could have high enough oxidation potentials to attack the polymer, but less than the 1.2 V needed to oxidize water.

The metal alloys presently used for pacing lead conductors, MP35N and Elgiloy, both contain cobalt. So far, a cobalt-free alloy has not been found that has adequate flex-life, conductivity, mechanical strength, and corrosion resistance. If such an alloy were developed, however, MIO

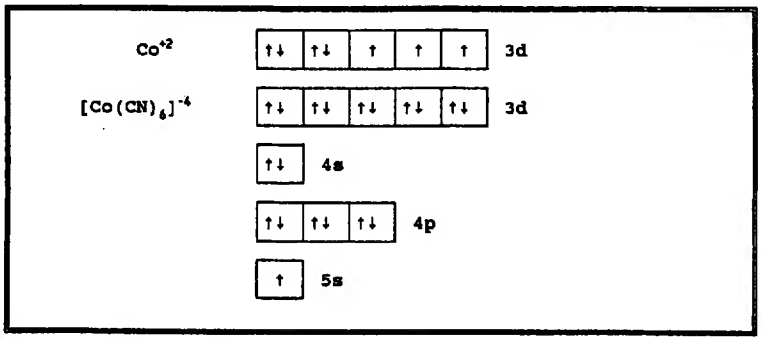

Figure 9. Schematic representation of the electronic configuration of the outer (transition) orbitals of the cobalt II ion. The top schematic represents a cobalt II ion in solution in distilled water. The bottom schematic shows how the oxidation potential of the ion can be increased significantly by complexation.

Figure 10. Scanning electron micrograph showing the surface of a Pellethane 2363-80A insulated cardiac pacing lead implanted in a canine for two years. The surface on the left was left undisturbed. That on the right was gently scraped with a scalpel. The surface shows infrared evidence of oxidation, especially with loss of PTMO ether at about 1075 cm^{-1} compared to urethane ether at about 1105 cm^{-1}.

resistance would not be assured, since we cannot rule out MIO by other transition metal ions. This is especially complicated by the fact that the oxidation state of the metal ion involved in MIO is unknown.

Surface Oxidation and Microcracking

Microscopic inspection of explanted polyether polyurethanes often reveals very shallow, random, brittle cracks on the surface (Figure 10). These cracks are only microns deep and do not seem to propagate deeper as a function of time. FTIR using ATR reveals that the polymer on the surface is in fact oxidized (Figure 11) [39]. It has been observed that the occurrence of this phenomenon decreases as the hardness of the polymer increases (the ether concentration decreases). Therefore, it is more prevalent on Pellethane 2363-80A than 55D surfaces, and has not been seen on Pellethane 2363-75D surfaces.

It is believed that this surface oxidation and microcracking is the result of direct exposure to the cellular components of the foreign body response [21,22,31–33]. The degradation is believed to follow the mechanisms outlined in Equations (7), (8), (10), and (11) through (25), above. We believe the oxidant is oxygen free radicals, such as $O_2^{\cdot}$ and $^{\cdot}OH$ released from cells on the device surface. Autoxidation is a diffusion limited process. In solids, autoxidation kinetics are not usually linear [30]. The initial "induction period" is followed by an autoacceleration phase where the bulk of the reaction occurs on and near the surface. The subsequent autoretardation phase can be attributed to the

need for the oxidant to permeate into the bulk to continue the reaction. If indeed this surface oxidation is the result of a reaction between polymer and oxygen free radicals, then diffusion of those free radicals into the bulk is highly improbable because of their high reactivity. It is, therefore, reasonable to expect that this surface reaction will slow markedly within a few microns of the surface, and possibly even terminate.

Environmental Stress Cracking (ESC)

Another failure mechanism that can affect implanted polyether polyurethanes has been termed environmental stress cracking (ESC). This is the generation of deep crazed cracks (see Figure 12) in response

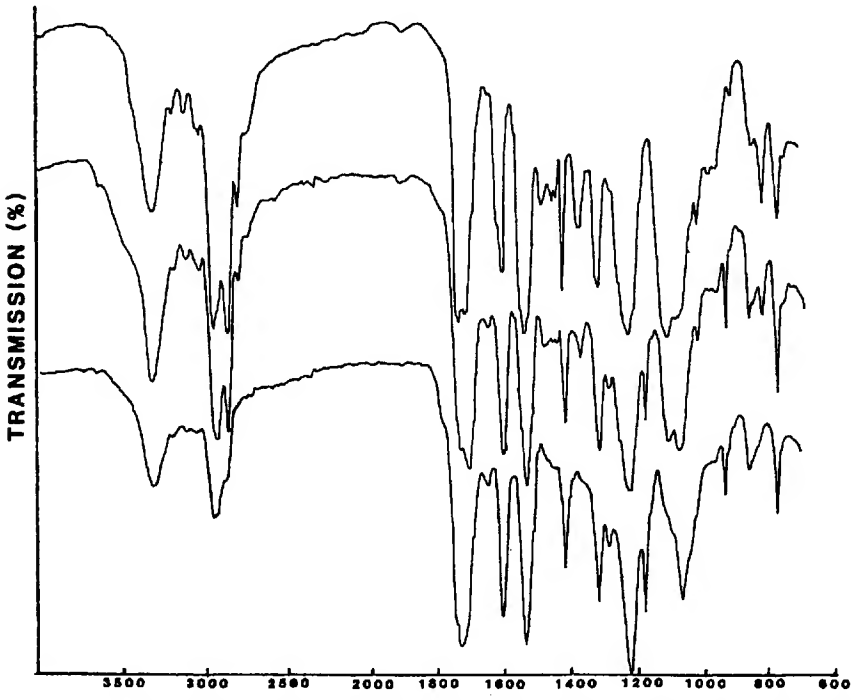

Figure 11. FTIR spectra comparing unimplanted Pellethane 2363-80A (top) with microcracked, tissue contacting surfaces (center) and polymer degraded within a tubular specimen in contact with a cobalt mandrel (bottom). Note the loss of the PTMO soft segment at about 1105 cm^{-1} relative to the urethane ether at about 1075 cm^{-1}. The loss of PTMO ether soft segment also affects the changes seen at about 2920 and 2850, 1730 and 1705, and 1401 to 1310 cm^{-1}.

Figure 12. A crazed crack in Pellethane 2363-80A typical of ESC (left) compared to brittle cracks resulting from MIO (right).

to residual stress and exposure to some chemical environment [40]. To be perfectly clear, the term "environmental" means that the chemical interactions are not yet clearly understood, and when they are, the mechanism can be more specifically named. At present, two theories have been proposed.

ESC Due to HOCl and NO_3 Released from PMNs

Sutherland, et al. proposes that ESC is the result of hypohalous and nitric oxide based oxidants resulting from activation of neutrophils, specifically polymorphonuclear leukocytes (PMNs), on the surface of the polymer [41]. A detailed analysis of their results is beyond the scope of this paper. However, at least one point needs to be emphasized. It has been well established that PMNs disappear within three days of surgical implant [22]. Monocytes are also present acutely, but because of their greater longevity, they predominate as the major cell type present three to seven days postimplant. Monocytes migrate into the implant site and differentiate into macrophages, which adhere to the surface of the implanted polyurethane within three days postimplant. These may further differentiate into foreign body giant cells on the surface of the

polymer. It is, in fact, the macrophage and foreign body giant cell that predominate on the surface of the implanted device chronically, not the PMN. This is important because while the reactive oxygen intermediates (such as superoxide anion and hydroxyl radical) and other agents produced by PMNs are also produced by macrophages, hypochlorous acid (HOCl) is not. The transcription of myeloperoxidase (which macrophages do not possess) is necessary for the production of HOCl. Sutherland, et al. did demonstrate the presence of myeloperoxidase on the surface of specimens after only twenty-four hours implant. While we can not rule out the possibility that there were PMNs on the surface, it is also possible that the enzyme resulted from contamination of the surface during explant and specimen debriding at a time when a high population of PMNs in the adjacent tissues is to be expected. Indeed, in our cage experiments, which preclude this probability, we have not seen PMNs settle on the material's surface. For this and other reasons (including different interpretation of infrared spectra), we suggest that the proposed ESC mechanism involving the release of HOCl and NO_3 on the surface of the specimens by PMNs is unlikely.

ESC as a Four Factor Interaction Involving the Foreign Body Response

Another theory to explain ESC is consistent with known inflammatory and foreign body response processes. We propose that ESC requires the interaction of at least four factors to occur *in vivo*. In all cases, so far, shallow surface autoxidation has been present on explanted, cracked samples. This oxidation always involves the loss of soft segment ether relative to the urethane ether. This is most notable in the loss of soft segment ether stretch at about 1105 cm^{-1} relative to the urethane ether stretch at about 1075 cm^{-1} (see Figure 11). Given that macrophages and foreign body giant cells reside on the surface of the implant, oxidation of the surfaces by oxygen free radicals is probable, possibly with some enzymatic assistance [14,21–29,31–33,39,40,42]. Oxidation of the surface of the polymer is not enough to produce ESC, however. Controlled studies of implants as a function of residual strain indicate that there is both an induction period and a critical strain, both symptomatic of stress cracking phenomena [40,41–45]. Factorial studies with Pellethane 2363-80A have demonstrated that the induction periods and critical strains can be significantly affected by manufacturing processes [40]. For example, annealing a sample to completely remove residual stress will prevent ESC (but not surface oxidation), provided that subsequent stress is not imposed by and during implant. Controlled animal studies have demonstrated that ESC decreases as the ether content decreases (hardness increases) [40].

Zhao, et al. have implicated certain proteins, particularly α_2-macroglobulin or ceruloplasmin, as probable catalysts or chain transfer agents which appear to facilitate crack development through the ether soft segment *in vivo* [42]. More recently, Zhao has been able to generate ESC-like cracks without proteins *in vitro* using continuously generated $O_2^{\cdot}$ and $^{\cdot}OH$, at a rate probably far beyond that possible *in vivo* [46]. Granted, some of this evidence is circumstantial. For example, just because oxidation of the surface has always been seen on cracked samples does not prove that it is a cause. It could be a result of cracking (since each polymer chain that breaks in tension produces two free radicals which can in turn generate many more free radicals, and initiate the autoxidation reaction) [14,47,48]. Because we have found ESC to vary as a function of ether content, this does not assure that ether-free polymers that we haven't studied yet won't crack. That said, our most current theory indicates that *in vivo* ESC requires the critical interaction between surface autoxidation, residual stress (strain), ether linkages and a proteinaceous crack driver.

If we assume that the above requirements for ESC are correct, then several possibilities exist for controlling or eliminating it [49]. A very shallow barrier coating on the surface should prevent surface oxidation and ESC because oxygen free radicals could not survive long enough to migrate through it, and it may be a barrier to α_2-macroglobulin. We have observed that very thin coatings of materials such as silicone rubber do indeed prevent surface oxidation and ESC [40]. Unfortunately, the adhesion of the coating in our testing was inadequate to assure reliability as a function of implant time. Annealing to remove residual stress (strain) has been a major factor in very significantly reducing ESC failures, but it is not 100% effective and cannot eliminate surface microcracking [40]. Even if the device is stress-free when it leaves the factory, it cannot be implanted stress-free, and the body does impose its own stresses. Of course, it is not possible to eliminate proteins by annealing. Thus, the one sure means of eliminating ESC (if our theory is correct) is to eliminate the ether linkage from the polymer, replacing it with one that is either oxidation resistant and/or not susceptible to interactions with crack-driving protein catalysts.

A Comparison of ESC and MIO

There does appear to be some confusion as to whether or not ESC and MIO are indeed the same mechanism. While both involve oxidation of the polyurethane's soft segment ether, the similarity stops there (see Table 1). For example, ESC occurs from the outer, tissue contacting surface of the polymer inward. It is the development of deep, rough or

Table 1. Some known and perceived factors affecting ESC and MIO in implanted polyurethanes.

ESC	MIO
Crazed cracks *in vivo* due to plastic deformation	Smooth cracks due to brittle deformation upon drying
Oxidized surfaces	Oxidized bulk
Requires cellular interactions	Does not appear to require cellular interactions
Requires residual strain	Does not require residual strain
Can be mitigated by annealing	Annealing of marginal to little help?
Appears to require α_2-macroglobulin, et al. to facilitate cracks *in vivo*	Requires cobalt corrosion products (initiates at metal-polymer contact points)
Cracks stabilize if residual stress relieved	Time dependent mechanism
Develops under fibrotic tissue	Fibrotic tissue not required
Can be prevented by thin silicone barrier coating	Thin silicone coating on polymer has no effect
Requires ether linkages	Any organic polymer may be susceptible

spiculated cracks derived from crazes which are typical of low rates of loading and plastic deformation (Figure 12) [50]. A craze ". . . is modeled as a collection of independent fibrils that draw from the substrate by a process akin to the drawing of textile fibres with necking" [51]. While autoxidation of surfaces appears to be involved, ESC per se (deep crazed cracks) occurs in response to residual stresses (strains). Without the residual strain, ESC does not occur. Autoxidation of the polymer appears to be limited to the tissue contacting surfaces and the crack faces. Autoxidation of the tissue contacting surfaces is the result of the foreign body response whereas that of the crack faces is certainly enhanced by chain cleavage [Equation (12)] [47,48]. In contrast, MIO is initiated at the interface between metallic parts and the polymer (within the device) and propagates outward. It is a *bulk* oxidation process which results in deep brittle (very smooth) cracks typical of low (below the glass transition) temperatures and/or a high rate of loading (Figure 12) [50]. Residual stress (strain) is not required for MIO cracking so that annealing may not significantly affect this mechanism. While it has been duplicated by soaking leads in 3% H_2O_2 at 37°C, it also has been observed *in vivo* in locations of very low oxygen tension and no evidence of a foreign body response (that is, no fibrous encapsulation, no cellular components on the surface). Thus, these facts combined with

other observations shown in Table 1 suggest that ESC and MIO are two different mechanisms, both involving oxidation (but not necessarily even the same oxidation mechanism).

Mineralization

Mineralization is the deposition of calcium containing apatitic mineral on or in an implanted device. Mineralization is generally subdivided into two categories, intrinsic and extrinsic. Intrinsic mineralization occurs within the boundaries of the biomaterial. This phenomenon has been observed in cardiac pacing leads only rarely. Extrinsic mineralization is associated with elements of tissue that were not initially implanted, such as thrombus, vegetations, necrotic tissue, very thick fibrotic capsules, etc. This is more commonly seen adjacent to leads that have been implanted in canines for longer periods and occasionally in adolescent humans.

The generally accepted theoretical mechanism for extrinsic mineralization is that cellular debris, surface defects, and/or relatively thick fibrous encapsulation of the device lead to nucleation of calcium phosphate deposition [20]. The salt deposits grow with time and eventually are transformed into apatite-like mineral. The extent of mineralization has been attributed to numerous factors. For example, the patient's age, but not necessarily the patient's immunological status appears to be important. Thus, devices implanted in pediatric patients run a relatively high risk of mineralization. Trapped and degraded cells in fibrous capsules can initiate mineralization if phagocytes are unable to reach and remove cellular debris. Factors such as cyclic stress, however, do not appear to be a significant part of the mechanism. As a result, the accepted means of screening polymers for mineralization is subcutaneous implant in adolescent rats [52].

A NEW POLYCARBONATE POLYURETHANE

A new polycarbonate polyurethane (see Figure 5) has excellent physical properties as shown in Table 2. It compares very favorably with its analogous Pellethane elastomers. ChronoFlex AL55D has a property that makes it very interesting for possible use in implantable cardiac pacing leads. Cardiac pacing leads must be advanced through portions of the venous system before final placement of the electrode(s) within the heart's right atrium or ventricle. A somewhat stiffer lead facilitates this maneuvering. Once placed, however, the lead should be as flexible as possible to reduce the risk of penetrating the myocardium, or dis-

Table 2. Mechanical and electrical properties of dry ChronoFlex AL55D and Pellethanes 2363-80A and 55D molded films (0.025 inches thick).

Property	ASTM D-	ChronoFlex AL55D	Pellethane 2363-80A	Pellethane 2363-55D
Young's modulus (psi)	1709	6,670 ± 1,560	2,650 ± 285	24,890 ± 2,760
100% modulus (psi)	1709	1,330 ± 88	824 ± 8	2,920 ± 75
300% modulus (psi)	1709	1,540 ± 66	585 ± 9	1,890 ± 780
Tensile strength (psi)	1709	7,160 ± 738	5,700 ± 460	7,560 ± 550
Elongation (%)	1709	400 ± 27	580 ± 22	350 ± 23
Tear strength (pli)	624	590 ± 35	456 ± 11	860 ± 46
Volume resistivity	257	9.4×10^{13}	4×10^{12}	6×10^{13}

lodging the tip. In the aromatic polyurethanes, hardness correlates (approximately) with elastic modulus. However, the same hardness in the aliphatic polyurethanes produces a lower elastic modulus. Molded ChronoFlex Al55D has an elastic modulus similar to Pellethane 2363-90A, which is stiffer than Pellethane 2363-80A but more flexible than Pellethane 2363-55D. ChronoFlex Al55D softens significantly after implant, becoming more like Pellethane 2363-80A in flexibility (see Table 3). Thus, this new polymer offers important property advantages for flexible implantable devices, but only if it is proven to be adequately biostable.

Hydrolytic Resistance

The hydrolytic stability of rigid polycarbonate is probably due to its low water permeability, which is attributed to the rigidity of the polymer chains. Increasing the flexibility of chains by copolymerization can increase water permeation and lower the stearic requirements for hydrolysis. Thus, polyethylene terephthalate (PET, a close relative of polycarbonate) is less hydrolytically stable under more severe, nonphysiologic conditions than polycarbonate. Under physiologic conditions, however, PET is considered to have adequate hydrolytic stability for extensive use in implanted woven or knitted fabrics. However, it is not a "given" that a polycarbonate polyurethane will be hydrolytically biostable, so this must be proven. So far, ChronoFlex AL55D has demonstrated no indications of hydrolytic degradation at all in our long-term *in vivo* qualification tests.

ESC Resistance

Since ChronoFlex Al55D can be considered ether-free, it should be ESC resistant if our theory is correct. A test has been designed to accelerate ESC *in vivo* using excessive strain as the accelerant [40]. Extruded tubing is stretched over 0.5 inch long, dumbbell shaped mandrels to 400% elongation. The strain is fixed at the ends with polyester suture. Other samples are mounted without stretching over similar mandrels while some unstretched tubing samples are filled with Medical Adhesive to keep pressure applied by tissue from collapsing it and imposing uncontrolled strain. Other specimens may be prepared using different compositions or manufacturing processes, such as annealing, solvent extraction, extrusion conditions, different strains, etc. The experimental specimens are implanted with controls in the dorsal

Table 3. Mechanical and electrical properties of saturated ChronoFlex AL55D and Pellethanes 2363-80A and 55D molded film (0.025 inches thick) after 1 week soak in 70°C saline.

Property	ASTM D-	ChronoFlex AL55D	Pellethane 2363-80A	Pellethane 2363-55D
Young's modulus (psi)	1709	3,190 ± 380	2,410 ± 357	9,450 ± 350
100% modulus (psi)	1709	760 ± 42	788 ± 21	2,030 ± 43
300% modulus (psi)	1709	680 ± 31	540 ± 10	1,530 ± 25
Tensile strength (psi)	1709	3,980 ± 140	4,380 ± 425	6,710 ± 374
Elongation (%)	1709	430 ± 12	560 ± 39	440 ± 15
Tear strength (pli)	624	390 ± 21	524 ± 41	770 ± 37
Volume resistivity (Ω − cm)	257	7.4×10^{13}	8×10^{10}	10^{12}

Table 4. Molecular weights and thermal transitions in ChronoFlex AL55D and Pellethanes 2363-80A and 55D molded films (0.025 inches thick).

	ASTM D-	ChronoFlex AL55D	Pellethane 2363-80A	Pellethane 2363-55D
$M_w \times 10^5$	3593	201,900 ± 5,100	339,000 ± 45,000	286,300
$M_n \times 10^5$		128,000 ± 3,490	224,000 ± 22,000	174,000
d		1.58 ± .001	1.50 ± .04	1.6
T_g (°C)	3418	−1 ± 2	−46 ± 1.5	—
T_m (°C)		121 ± 0.5	130 ± 3	178 ± 2
dH (J/g)		1.5 ± 0.4	1.8 ± .6	15 ± 1

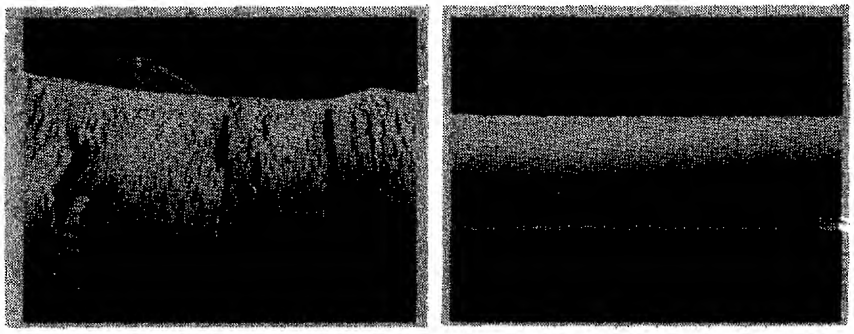

Figure 13. SEM micrographs showing typical *twelve week* ESC results of 400% elongated, unannealed ChronoFlex AL55D (left) and unannealed Pellethane 2363-80A (right).

subcutis of rabbits. Specimens are typically explanted at twelve weeks for screening studies, but some implants have continued for as long as two years. Six months appears to be evolving as a standard [53].

The polycarbonate polyurethane, ChronoFlex AL55D, exhibits no evidence of ESC at all in our twelve week screening test, even at 400% elongation, unannealed (Figure 13). Unannealed Pellethane 2363-80A is severely degraded in this test, however. Other polymers that have demonstrated equivalent or worse ESC degradation in this test include Tecothane 80A (structurally similar to Pellethane 2363-80A), Surethane (apparently structurally similar to Biomer)®, and TecoFlex EG80A. While Pellethane 2363-55D is rather stiff for cardiac pacing leads, it is used because of its improved biostability (typically no ESC is seen in the twelve week test). TecoFlex EG60D shows no ESC in twelve weeks at lower elongations ($\leq$300%), but does crack at 400% elongation. Thus, ChronoFlex AL55D appears to have excellent ESC resistance in screening tests, as do some of the stiffer polyether polyurethanes.

In eighteen month implants, unannealed ChronoFlex Al55D continues to show no signs of ESC at 400% elongation (Figure 14). In comparison, about 50% of annealed 400% elongated Pellethane 2363-80A specimens develop shallow microcracking (Figure 14). This is usually not accompanied by the deep cracks seen in the unannealed polymer (Figure 13). Under the same conditions, Pellethane 2363-55D specimens also typically exhibit no ESC in eighteen months, as shown in

---

Biomer® is a registered trademark of Cardiac Control Systems.

Figure 14. Thus, our preliminary conclusion is that the aliphatic polycarbonate polyurethane, ChronoFlex AL55D, is at least equivalent (and possibly superior) to its aromatic Shore 55D polyether analogues *and* has superior mechanical flexibility.

MIO Resistance

In vitro screening tests have been done by immersing metal conductor coil/tubing subassemblies (resembling cardiac lead bodies) in 3%, 37°C H_2O_2 in polyethylene or other nonreactive containers [54]. The H_2O_2 is changed three times per week to assure activity. The transition metals, cobalt and molybdenum, produce severe degradation of Pellethane 2363-80A and Surethane (Biomer). Cobalt and molybde-

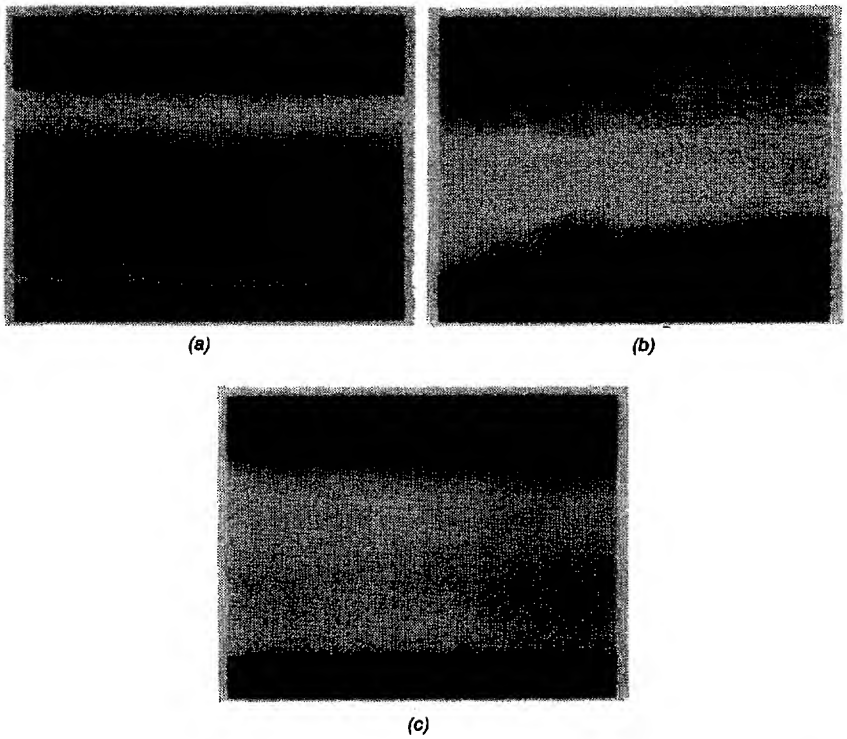

Figure 14. SEM micrographs showing typical *eighteen month* ESC results of 400% elongated polyurethanes: (a) ChronoFlex AL55D–typical of all surfaces, (b) annealed Pellethane 2363-80A–shallow cracks found on some surfaces, (c) annealed Pellethane 2363-55D.

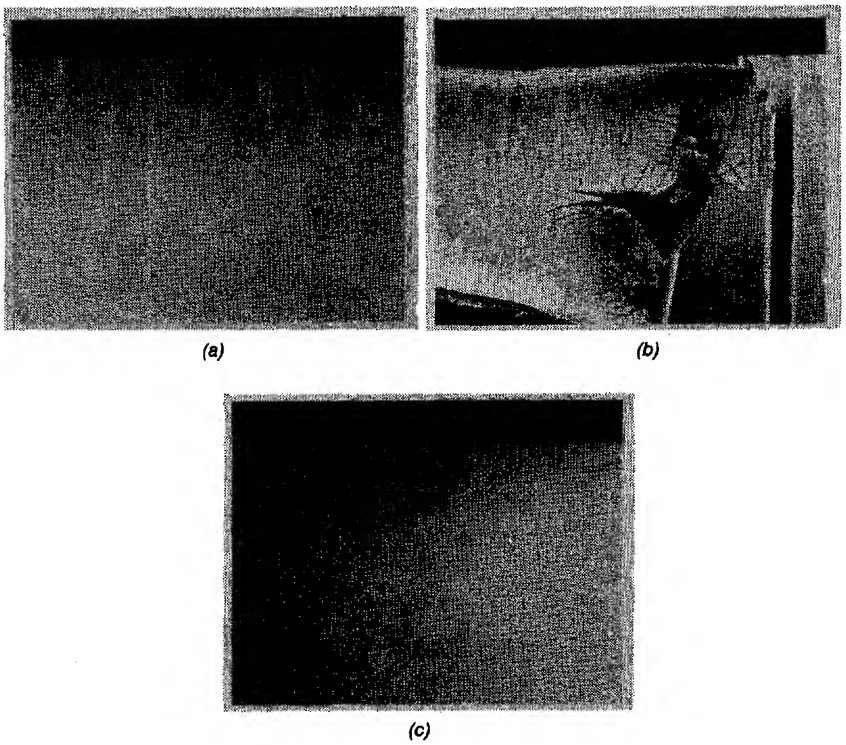

Figure 15. SEM micrographs showing the lumen surface of tubing after eighteen months implant in the presence of cobalt rod: (a) ChronoFlex AL55D–typical of all samples. The stripes are deposits between the grooves in the mandrel. There are no cracks; (b) Pellethane 2363-80A–typical of some surfaces; and (c) Pellethane 2363-555D.

num bearing alloys produce slower and less severe damage. Thinner polyether polyurethane tubing walls produce faster degradation, and MIO tends to decrease as the polymer's hardness increases. Pellethane 2363-55D, therefore, experiences less damage over a longer period of time than P80A for a given thickness in these tests. However, P55D is not immune to MIO, especially if used in thin sections. In this type of *in vitro* test, ChronoFlex Al55D has exhibited no MIO at all in the presence of MP35N or platinum coated MP35N (both used in wires in cardiac pacing leads).

In vivo, polyurethane MIO has only been seen to occur in the presence of cobalt and cobalt bearing alloys. Thus, pure cobalt mandrels have been used to accelerate *in vivo* MIO. Extruded tubing was placed over 0.5 inch long Co mandrels and controls. Strings of specimens were im-

planted in the dorsal subcutis of rabbits, then were explanted as a function of time for microscopic examination and other analysis (such as FTIR, GPC molecular weight distribution, etc.). About 50–60% of Pellethane 2363-80A specimens demonstrate microscopic evidence of MIO within twenty-four months implant. So far, no MIO has been observed in ChronoFlex AL55D (Figure 15).

Implanted Microtensile Specimens

There has been no evidence of degradation after eighteen months implant of 0.025 inch thick ChronoFlex AL55D microtensile specimens in the subcutis of rabbits. Completely reversible mechanical changes due to the absorption of a small amount of moisture have been noted. No evidence of mineralization was seen in subcutaneous implants in adolescent rats.

Implanted Cardiac Pacing Leads

After eighteen months implant, ChronoFlex AL55D insulated leads have excellent durability as far as can be told from noninvasive tests. It will require completion of the two year tests to determine how they compare with the implanted Pellethane 2363-80A control devices.

SUMMARY AND CONCLUSIONS

Polyurethane elastomers have property combinations that make them uniquely suited for use in long-term implanted biomedical devices. While certain polyether polyurethanes have been used successfully as neurologic and cardiac pacing lead insulation and connector modules for nearly twenty years, some problems have occurred. The softer versions are susceptible to *in vivo* stress cracking and oxidative phenomena. While the more rigid polymers are more biostable, they are also too stiff for many needed devices. Polyester polyurethanes, such as those used until only recently as coverings for implanted breast prostheses are subject to hydrolytic degradation. Therefore, until a means can be found to assure greater biostability in the softer grades of polyurethane elastomers, their tremendous potential will not be reached. While durable, small, slippery, tough cardiac and neurologic pacing leads can be made from polyether polyurethanes, their use in other devices such as leaflet valves and small diameter vascular grafts have not been successful. Significant progress is being made to completely understand ESC and MIO failure mechanisms with the goal of

developing more biostable materials. At present, at least one new polycarbonate polyurethane offers great promise as a long-term biostable elastomer with superior mechanical and biologic properties. If it does indeed continue to exhibit the excellent performance seen so far in qualification studies, then a new age of biomedical device development will become possible.

REFERENCES

1. "Market Study–Biomaterials Supply for Permanent Medical Implants," prepared for the Health Industry Manufacturers Association by Arnoff Associates, New York, March 1994.
2. Thermedics, Inc. Tecoflex Medical Grade Aliphatic Thermoplastic Polyurethanes (technical product information).
3. Thermedics, Inc. Tecothane Medical Grade Aromatic Thermoplastic Polyurethanes, Rev. 2/8/93 (technical product information).
4. Szycher, M. and A. M. Reed. Biostable Polyurethane Products, U.S. patent 5,254,662, October 19, 1993.
5. Pinchuck, L. Crack Resistant Polycarbonate Urethane Polymer Prostheses, U.S. patents 5,133,742 and 5,229,431, 1992 and 1993.
6. Bonart, R. J. 1968. *Macromol. Sci. Phys.,* 32:115.
7. Lelah, M. D. and S. L. Cooper. 1986. "Stability," in *Polyurethanes in Medicine,* Boca Raton: CRC Press, pp. 201–209.
8. Mirkovitch, V., M. J. Akutsu and W. J. Wolf. 1962. "Polyurethane Aorta in Dogs, Three-Year Results," *Trans. ASAIO,* 8:79.
9. Boretos, J. 1972. "Tissue Pathology and Physical Stability of a Polyether Elastomer on Three-Year Implantation," Communication to the editor, *J. Biomed. Mater. Res.,* 6:473–476.
10. Boretos, J., W. Pierce, R. Baier, A. LeRoy and M. Donachy. 1975. "Surface and Bulk Characterization of a Polyether Urethane for Artificial Hearts," *J. Biomed. Mater. Res.,* 9:327–340.
11. Brash, J., B. Fritzinger and S. Bruck. 1975. "Development of Block Copolyether-Urethane Intra-Aortic Balloons and Other Medical Devices," *J. Biomed. Mater. Res.,* 7:313–334.
12. Stokes, K., K. Cobian and T. Lathrop. 1979. "Polyurethane Insulators, A Design Approach to Small Pacing Leads," in *Proceedings of the VIth World Symposium on Cardiac Pacing,* C. Meere, ed., Montreal: PACESYMP, 28-2.
13. Stokes, K. and K. Cobian. 1982. "Polyether Polyurethanes for Implantable Pacemaker Leads," *Biomaterials,* 3:225–231.
14. Stokes, K. 1988. "Polyether Polyurethanes: Biostable or Not?" *Biomater. Appl.,* 3:228–259.
15. Guyton, A. C. 1991. "The Body Fluid Compartments: Extracellular and Intracellular Fluids; Interstitial Fluid and Edema," *Textbook of Medical Physiology,* Philadelphia: W. B. Saunders Co., pp. 274–285.
16. Gesner, B. D. 1972. "Stabilization Against Chemical Agents," in *Polymer*

Stabilization, W. L. Hawkins, ed., New York: Wiley-Interscience, pp. 360–364.

17. Prafulla, A., J. Wille, K. Shah and A. Kydonieus. 1993. "Analysis of the Extractive and Hydrolytic Behavior of Microthane Poly(ester-urethane) Foam by High Pressure Liquid Chromatography," *J. Biomed. Mater. Res.,* 27:655–666.
18. Batich, C., J. Williams and R. King. 1989. "Toxic Hydrolysis Products from a Biodegradable Foam Implant," *J. Biomed. Mater. Res.,* 23(A3 Suppl.):311–319.
19. Szycher, M. and A. Siciliano. 1991. "An Assessment of 2,4 TDA Formation from Surgitek Polyurethane Foam under Simulated Physiological Conditions," *J. Biomater. Appl.,* 5:323–336.
20. Schoen, F. J., H. Harasaki and K. M. Kim et al. 1988. "Biomaterial-Associated Calcification: Pathology, Mechanisms, and Strategies for Prevention," *J. Biomed. Mater. Res.,* 22(A1 Suppl):11–36.
21. Anderson, J. M. 1988. "Inflammatory Response to Implants," *ASAIO,* II(2):101–107.
22. Anderson, J. 1993. "Mechanisms of Inflammation and Infection with Implanted Devices," *Cardiovasc. Pathol.,* 2(3 Suppl.):33S–41S.
23. Sibille, Y. and H. V. Reynolds. 1990. "Macrophages and Polymorphonuclear Neutrophils in Lung Defense and Injury," *Am. Rev. Respir. Dis.,* 141:471–501.
24. Angeline, B. D., A. Hiltner and J. M. Anderson. 1990. "Long-Term *in vitro* Enzymatic Biodegradation of Pellethane 2363-80A: A Mechanical Study," in *Degradable Materials: Perspectives, Issues and Opportunities,* S. A. Barenberg, J. L. Brash, R. Narayan and A. E. Redpath, eds., Boca Raton: CRC Press, pp. 295–322.
25. Ratner, B. D., K. W. Gladhil and T. A. Horbett. 1988. "Analysis of *in vitro* Enzymatic and Oxidative Degradation of Polyurethanes," *J. Biomed. Mater. Res.,* 22:509–527.
26. Phua, S. K., E. Castillo and J. M. Anderson et al. 1987. "Biodegradation of a Polyurethane *in vitro*," *J. Biomed. Mater. Res.,* 21(2):231–246.
27. Smith, R., D. F. Williams and C. Oliver. 1987. "The Biodegradation of Poly(ether) Urethanes," *J. Biomed. Mater. Res.,* 21:1149–1166.
28. Wasserbauer, R., M. Beranova and D. Vancurova et al. 1990. "Biodegradation of Polyethylene Foils by Bacterial and Liver Homogenates," *Biomaterials,* 11(1):36–40.
29. Beranova, M., R. Wasserbauer and D. Vancurova et al. 1990. "Effect of Cytochrome P-450 Inhibition and Stimulation on Intensity of Polyethylene Degradation in Microsomal Fraction of Mouse and Rat Livers," *Biomaterials,* 11(7):521–524.
30. Hawkins, W. L. 1972. *Polymer Stabilization,* New York: Wiley-Interscience.
31. Zhao, Q., M. P. Agger, M. Fitzpatrick and J. M. Anderson et al. 1990. "Cellular Interactions with Biomaterials: *In vivo* Cracking of Pre-Stressed Pellethane 2363-80A," *J. Biomed. Mater. Res.,* 24:621–637.
32. Zhao, Q., N. Topham, J. M. Anderson et al. 1991. "Foreign-Body Giant

Cells and Polyurethane Biostability: *In vivo* Correlation of Cell Adhesion and Surface Cracking," *J. Biomed. Mater. Res.*, 25:177–183.

33. Anderson, J. M., A. Hiltner and Q. H. Zhao et al. 1992. "Cell/Polymer Interactions in the Biodegradation of Polyurethanes," in *Biodegradable Polymers and Plastics,* M. Vert, J. Feijen and A. Albertsson et al., Cambridge, England: Royal Society of Chemistry, pp. 122–136.
34. Stokes, K., P. Urbanski and J. Upton. 1990. "The *in vivo* Auto-Oxidation of Polyether Polyurethanes by Metal Ions," *J. Biomater. Sci. Polym. Edn.*, 1(3):207–230.
35. Ranby, B. and J. F. Rabek. 1975. "The General Mechanism of Oxidation of Polymers," in *Photodegradation, Photo-Oxidation and Photostabilization of Polymers,* London: Wiley, Chapter 3.
36. Coury, A., P. Cahalan, E. Schultz et al. 1984. *In vitro* Aging of Implantable Polyurethanes in Metal Ion Solutions," *Trans Second World Congress on Biomater.*, p. 252.
37. Weast, R. C. and M. J. Astle. 1978–79. *CRC Handbook of Chemistry and Physics, 59th Edition.* Boca Raton: CRC Press, PD193 (and Hodgman, C. D., R. C. Weast and S. M. Selby, 39th Edition)..
38. Thoma, R. J. and R. E. Phillips. 1988. "Ionic Interactions of Polyurethanes," *J. Biomater. Appl.*, 3:180–205.
39. Wu, Y., C. Sellitti, J. M. Anderson, A. Hiltner, G. A. Lodoen and C. R. Payet. 1992. "An FTIR-ATR Investigation of *in vivo* Poly(ether urethane) Degradation," *J. Appl. Pol. Sci.*, 46:201–211.
40. Stokes, K., P. Urbanski and K. Cobian. 1987. "New Test Methods for the Evaluation of Stress Cracking and Metal Catalyzed Oxidation in Implanted Polymers," in *Polyurethanes in Biomedical Engineering II,* H. Planck, et al., eds., Amsterdam: Elsevier, pp. 109–128.
41. Sutherland, K., J. R. Mahoney, A. J. Coury and J. W. Eaton. 1993. "Degradation of Biomaterials by Phagocyte-Derived Oxidants," *J. Clin. Invest.*, 92:2360–2367.
42. Zhao, Q. H., A. K. McNally, K. R. Rubin, M. Renier, Y. Wu, V. Rose-Caprara, J. M. Anderson, A. Hiltner, P. Urbanski and K. Stokes. 1993. "Human Plasma $Alpha_2$-Macroglobulin Promotes *in vitro* Oxidative Stress Cracking of Pellethane 2363-80A. *In vivo* and *in vitro* Correlations," *J. Biomed. Mater. Res.*, 27:379–389.
43. Stokes, K., W. A. Frazer and E. A. Carter. 1984. "The Biostability of Various Polyether Polyurethanes under Stress," *ANTEC '84,* pp. 1073–1075.
44. Wu, Y. K., G. A. Lodoen, J. M. Anderson, E. Baer and A. Hiltner. 1994. "Creep of a Poly(etherurethane urea) in an Oxidative Environment," *J. Biomed. Mater. Res.*, 28:515–522.
45. Wu, Y. K., K. R. Sletten, V. Topolkaraev, G. A. Lodoen, J. M. Anderson, E. Baer and A. Hiltner. 1994. "Effect of an Oxidative Environment on the Creep Compliance of Poly(ether Urethane Urea)," *J. Biomed. Mater. Res.*, 53:1037–1049.
46. Zhao, Q., J. Casas-Bejar, P. Urbanski and K. Stokes. "The Glass Woll-$H_2O_2/CoCl_2$ Test System for *in vitro* Evaluation of Biodegrative Stress

Cracking in Polyurethane Elastomers," accepted for publication in *J. Biomed. Mater. Res.*

47. Bresler, S. E., S. N. Zhurkof and E. N. Kasbekov. 1959. "Investigation of Macroradicals Formed during the Mechanical Destruction of Polymers," *Techn. Fiz.*, 321–325.
48. Gent, A. N. and C. T. R. Pulford. 1984. "Micromechanics of Fracture in Elastomers," *Journal of Materials Science*, 19:3621–3619.
49. Wu, Y., Q. Zhao, J. M. Anderson, A. Hiltner, G. A. Loedoen and C. R. Payet. 1991. "Effect of Some Additives on the Biostability of a Poly(etherurethane) Elastomer," *J. Biomed. Mater. Res.*, 25:725–739.
50. Peterlin, A. 1970. "Chain Scission and Plastic Deformation in the Strained Crystalline Polymer," *J. Pol. Sci.*, 32:297–317.
51. Passaglia, E. 1984. "Distribution of Stress in a Craze of the Tip of a Uniformly Extended Crack," *Polymer*, 25(12):1727–1733.
52. Fishbein, M., R. J. Levy and N. A. Ferrans et al. 1982. "Calcification of Cardiac Valve Bioprostheses; Biologic, Ultrastructural, and Biochemical Studies in a Subcutaneous Implantation Model System," *J. Thorac. Cardiovasc. Surg.*, 83:602.
53. Draft HIMA protocol for the qualification of polyurethane elastomers.
54. Stokes, K. B., W. A. Berthelsen and M. W. Davis. 1985. "Metal Catalyzed Oxidative Degradation of Implanted Polyurethane Devices," *Proceedings of the ACS, Division of Polymeric Materials Science and Engineering*, 53, 6–10.